7-3-2013

Integration of a Sedimentation Module to a Hydrologic Model and its Application to a Mercury TMDL Analysis

Lilian Marrero
lmarr001@fiu.edu

DOI: 10.25148/etd.FI13080913

FLORIDA INTERNATIONAL UNIVERSITY

Miami, Florida

INTEGRATION OF A SEDIMENTATION MODULE TO A HYDROLOGIC MODEL AND ITS APPLICATION TO A MERCURY TMDL ANALYSIS

A thesis submitted in partial fulfillment of the

requirements for the degree of

MASTER OF SCIENCE

in

CIVIL ENGINEERING

by

Lilian Marrero

2013

To: Dean Amir Mirmiran
College of Engineering and Computing

This thesis, written by Lilian Marrero, and entitled Integration of a Sedimentation Module to a Hydrologic Model and Its Application to a Mercury TMDL Analysis, having been approved in respect to style and intellectual content, is referred to you for judgment.

We have read this thesis and recommend that it be approved.

_____
Georgio Tachiev

_____
Omar I. Abdul-Aziz

_____
Hector R. Fuentes, Major Professor

Date of Defense: July 3, 2013

The thesis of Lilian Marrero is approved.

_____
Dean Amir Mirmiran
College of Engineering and Computing

_____
Dean Lakshmi N. Reddi
University Graduate School

Florida International University, 2013

ACKNOWLEDGMENTS

This research work has been financially supported by the DOE-FIU Science & Technology Workforce Initiative developed by the US Department of Energy's Environmental Management (DOE-EM) and Florida International University's Applied Research Center (FIU-ARC). The FIU Department of Civil and Environmental Engineering provided the curricular and research framework to complete my MS degree in Civil Engineering. My gratitude goes to the committee members, Dr. Hector R. Fuentes, Dr. Georgio Tachiev, and Dr. Abdul-Aziz. Dr. Fuentes has always gone above and beyond the responsibilities of professor and served as a mentor throughout my undergraduate and graduate education at FIU. He provided valuable advice in the scientific and engineering aspects of the study, assessment approaches and written and oral presentation formats and quality. Dr. Georgio Tachiev has played an invaluable role in completing this thesis. His technical expertise, guidance, motivation, mentorship and availability to provide routine assistance ensured the successful completion of this research in a timely manner. I also thank Dr. Abdul-Aziz for serving on the committee and providing valuable critique in support of the model amendment to the mercury fate representation.

I wish to extend my gratitude to Dr. Leonel Lagos for his administration of the DOE fellowship program that supported me while completing my MS degree program and for always being an advocate of the great work performed by the DOE Fellows. Clint Miller and Angelique Lawrence have also been key assets to have within the ARC family.

I would like to thank my parents Libia and Edel Marrero for their unconditional love and unwavering support towards my professional and personal endeavors. I am

appreciative of the wisdom they have shared throughout the years. I cannot conclude without thanking my purest love and younger brother Steve Marrero for accepting and understanding my demanding graduate student schedule.

Once a DOE Fellow, always a DOE Fellow.

ABSTRACT OF THE THESIS

INTEGRATION OF A SEDIMENTATION MODULE TO A HYDROLOGIC MODEL AND ITS APPLICATION TO A MERCURY TMDL ANALYSIS

by

Lilian Marrero

Florida International University, 2013

Miami, Florida

Professor Hector R. Fuentes, Major Professor

This research is part of continued efforts to correlate the hydrology of East Fork Poplar Creek (EFPC) and Bear Creek (BC) with the long term distribution of mercury within the overland, subsurface, and river sub-domains. The main objective of this study was to add a sedimentation module (ECO Lab) capable of simulating the reactive transport mercury exchange mechanisms within sediments and porewater throughout the watershed. The enhanced model was then applied to a Total Maximum Daily Load (TMDL) mercury analysis for EFPC. That application used historical precipitation, groundwater levels, river discharges, and mercury concentrations data that were retrieved from government databases and input to the model. The model was executed to reduce computational time, predict flow discharges, total mercury concentration, flow duration and mercury mass rate curves at key monitoring stations under various hydrological and environmental conditions and scenarios. The computational results provided insight on the relationship between discharges and mercury mass rate curves at various stations throughout EFPC, which is important to best understand and support the management mercury contamination and remediation efforts within EFPC.

TABLE OF CONTENTS

LIST OF TABLES

TABLE PAGE

LIST OF FIGURES

FIGURE PAGE

LIST OF ACRONYMS AND ABBREVIATIONS

ARC	Applied Research Center
BC	Bear Creek
CI	Confidence Interval
DHI	Danish Hydraulic Institute
DOE	Department of Energy
EFPC	East Fork Poplar Creek
EPA	Environmental Protection Agency
OREIS	Oak Ridge Environmental Information System
ORNL	Oak Ridge National Laboratory
ORR	Oak Ridge Reservation
PPT	Parts Per Trillion
ROD	Record of Decision
RMSE	Root Mean Square Error
TMDL	Total Maximum Daily Load
TSS	Total Suspended Solids
UEFPC	Upper East Fork Poplar Creek
USGS	United States Geologic Survey
Y-12	Y-12 National Security Complex

LIST OF VARIABLES

A_{fl}	Cross sectional area
AD_c	ECO Lab advection-dispersion coefficient
adss	Adsorption
c	ECO Lab concentration
C	Soil water capacity
dess	Desorption
difv	Diffusion transfer coefficient in water
dz	Computational grid layer thickness
dzds	Thickness of diffusion layer in sediment
dzwf	Average thickness of water film through which metals diffuse
D_x, D_y, D_z	Dispersion coefficients in the x,y, and z-direction
$f_{biot \cdot difw}$	Factor for diffusion due to bioturbation
h	Flow depth or hydraulic head
k_a	Adsorption rate [d^{-1}]
K_d	Mercury partitioning coefficient between particulate matter and water
K_{ds}	Mercury partitioning coefficient between sediment and pore water
K_s	Saturated hydraulic conductivity
k_s	Desorption rate in sediment [d^{-1}]
k_w	Desorption rate [d^{-1}]
M	Manning's M, the reciprocal of Manning's n (1/n)
P_c	ECO Lab processes
pors	Porosity of sediment

PPR	Particle production rate [g/m^{2}d]
q	Volumetric flow or discharge
resv	Resuspension
RR	Resuspension rate [g/m^{2}d]
S	Specific storage coefficient
S_c	ECO Lab sources and sinks
sev	Sedimentation
S_{fx}, S_{fy}	Friction slopes in x and y-direction
S_{HM}	Dissolved mercury concentration in water
S_{HMS}	Dissolved mercury concentration in sediment pore water
t	Time
TSS	Total suspended solids concentration
u, v, w	Flow velocities in the x, y, and z-direction
uh, vh	Discharge per unit length in x and y-direction
v_s	Settling velocity [m/d]
v_c	Critical current velocity for initiation of the movement [m/s]
X_{HM}	Adsorbed mercury concentration in suspended matter
X_{HMS}	Adsorbed mercury concentration in sediment
X_{SED}	Mass of sediment
Z	Ground surface elevation

1. INTRODUCTION

The United States Department of Energy (DOE) decontamination and decommissioning activities of industrial, radiological and nuclear facilities seeks to restore the environmental conditions of contaminated sites to accepted levels designated by local, state and federal regulations. The East Fork Poplar Creek (EFPC) Watershed, shown in Figure 1, is located in the state of Tennessee and represents one of several DOE sites for which the mission of remidiation is of extreme importance. The Oak Ridge Reservation (ORR) has been on the Comprehensive Environmental Response, Compensation, and Liability Act National Priorities List since November 21, 1989 [**1**]. Upper EFPC (UEFPC) is subject to a complex array of contamination sources including but not limited to uranium, nitrate, boron, cadium, chromium, polychlorinated biphenyls, and volatile organic compounds such as trichloroethene, tetrachloroethane, and 1,2,-dichloroethene [**2**]. Mercury contamination is the focus of this study.

EFPC has been severely impacted by the release of more than 100 metric tons of elemental mercury as a byproduct of nuclear processing activities employed in the lithium-isotope separation process used in the production of nuclear fusion weapons during the 1950's [**3**] [**2**]. Contamination was introduced into groundwater through multiple paths including historical spills, pipeline leaks, and dissolution from contaminated soils and sediments and is still present in the watershed surrounding the Y-12 National Security Complex (Y-12) [**4**] [**5**]. The Tennessee Valley Authority estimated that floodplain sources contributed an estimated 80% of the total annual mercury from

the EFPC system [**6**]. Studies have identified over 77,000 kg of mercury present in the upper 10 feet of soils along a 15-mile long stretch of EFPC [**5**].

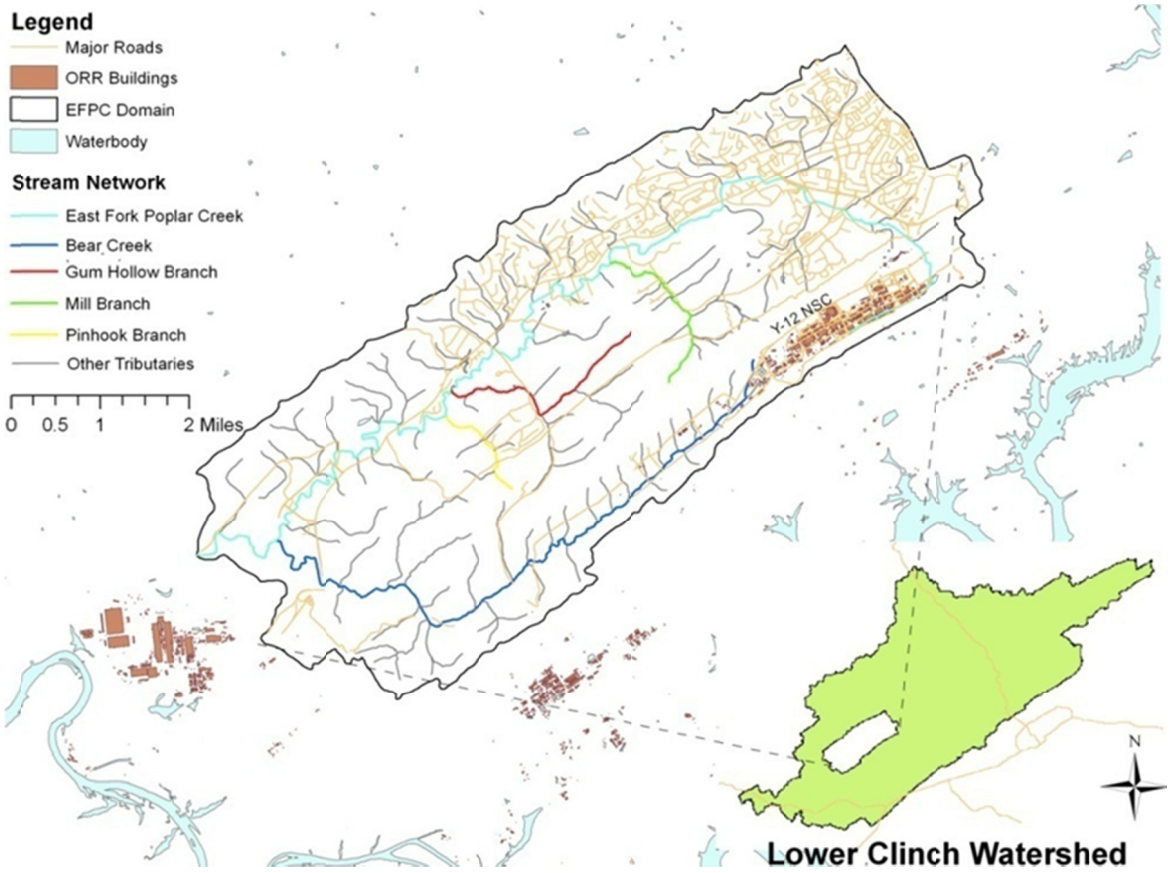

Figure 1. East Fork Poplar Creek watershed and stream network.

Figure 2. Mercury present in sub-surface soil samples from Oak Ridge [7].

Mercury is present in the sediment, surface water, groundwater, and infrastructure in the Y-12 area and in the upper reaches of EFPC [**5**]. Mercury releases into the creek ceased in 1963 [**8**]. Nonetheless, although remediation strategies have been implemented since the problem's inception, the issue of mercury contamination continues to prevail. Even though water quality has been improved by remediation strategies, methyl mercury concentrations in water and in fish have not decreased and in some cases exhibit trends of increasing concentration [**8**].

The state of Tennessee continues to list portions of EFPC as not supporting their designated use classifications, such as aquatic life, irrigation, livestock watering, wildlife, and recreation due to mercury contamination [**9**]. Streams and lakes in violation of one or more water quality standards within the state of Tennessee are described in list 303 (d). Portions of this list are summarized in the table below for streams near ORR. Shown in Table 1, contaminated streams relevant to the present study include 9.7 impaired miles of EFPC within Roane County, and 11.3 miles within Anderson and Roane. Approximately 141 acres of the Poplar Creek Embayment, Watts Bar Reservoir, within Roane County are also contaminated. Total Maximum Daily Load (TMDL) studies identify the sources of pollutant in a stream, quantify the amount, and recommend appropriate action to be taken in order for the stream to no longer be polluted. Further analysis and modeling of the area is necessary so that TMDL studies may be developed in the future.

Elemental mercury dissolves and oxidizes to mercuric ion under environmental conditions, resulting in increased mobility of mercury due to its increased solubility. Due to its highly stable complex formations often considered as irreversible forms and its strong binding to high affinity environments, mercury is often regarded as highly

immobile in soils [**10**]. Higher concentrations of mercury and suspended solids have been recorded as a byproduct of higher volumes and higher stream velocities during and post flood events [**11**]. Generally in stratified systems, concentrations of total mercury and methyl mercury are higher near the sediments [**12**]. The kinetics of mercury with dissolved organic matter in aquatic ecosystems requires additional evaluation as the dominant complexes are difficult to determine [**13**].

Table 1. Streams in violation of water quality standards.

Water Body ID	Waterbody Impacted	County	Miles/Acres Impaired
TN06010207026 – 0600	Bear Creek	Roane	10.87
TN06010207026 – 1000	EFPC	Roane	9.7
TN06010207026 – 2000	EFPC	Anderson/Roane	11.3
TN08010208009 - 1000	Poplar Creek	Haywood/Fayette	23.6
TN08010208011 - 2000	Bear Creek	Fayette	7.9
TN08010209021 – 0110	Bear Creek	Shelby/Tipton	14.5
TN05130104050 - 0100	East Branch Bear Creek	Scott	5.7
TN05130104050 - 1000	Bear Creek	Scott	2.6
TN06010102003 – 0500	Bear Creek	Sullivan	4.6
TN08010204004 - 0100	Bethel Branch	Dyer/Gibson	30.4
TN06010207001 - 0100	Poplar Creek Embayment, Watts Bar Reservior	Roane	141 ac

Mercury present in surface water is converted to various forms. Mercury particles may settle with sediments, may be consequently diffused into the water column, resuspended, or hidden within sediments until a hydrological event disturbs the particles and reignites the complex cycle through which it is recycled [**11**]. Mercury in the sediment column may be released into the water via remobilization, dissolution and desorption; and subsequently bio-accumulated by aquatic organisms [**14**]. Mercury is released from bed sediments as bed layer particles are resuspended. Mercury exchange occurs between the water column and sediment as well as between the dissolved and adsorbed phases of mercury via adsorption-desorption processes [**15**]. Mercury

contamination in the environment represents a health concern for wildlife, as well as humans [**16**]. Studies have shown a correlation between total mercury concentration within the creek and methyl mercury concentrations and long-term bio accumulation and magnification. Another mercury study revealed a positive trend among increases in total mercury and methyl mercury, and increases in organic carbon [**17**] [**18**]. Methyl mercury is the most toxic form of mercury because it can accumulate at a faster rate within organisms in comparison to the rate at which it can be eliminated; it takes longer for organisms to remove it from their systems [**16**]. Effects are dependent upon the chemical form and type of exposure. The mercury within the EFPC system is continuously recycled by the surrounding environment, making the successful implementation of remediation strategies difficult to execute. The irreversibility of mercury adsorption-desorption on soils involves complex mechanisms [**19**]. Understanding the processes by which mercury is transported and recycled within the EFPC environment is an essential step towards complying with applicable and relevant or appropriate requirements in the DOE's Record of Decision (ROD) Phase I and Phase II [**20**] [**21**].

1.1 Site Description

The geological characteristics of the EFPC watershed have been extensively explored by past remedial investigations for the site [**22**]. Tributaries' attributes and vegetation cover have also been described in great detail by Long [**23**]. This section serves as a summary of efforts previously executed in characterizing the site.

EFPC is located within the ORR in the state of Tennessee, in the counties of Roane and Anderson. The reservation houses three major US DOE facilities within 14,260 ha. These include Y-12, the East Tennessee Technology Park or K-25 complex, and the Oak Ridge National Laboratory (ORNL). EFPC watershed is a sub-watershed of the larger Poplar Creek watershed. The United States Geologic Survey (USGS) classifies it as one of four sub-watersheds of the Lower Clinch River watershed (Hydrologic Unit Code 06010207). The EFPC watershed domain area covers approximately 29.7 square miles.

An estimated 88 square miles of streams and tributary branches have been identified within the domain. Bear Creek (BC) and EFPC are two small rivers with a length of more than 12,500 kilometers. As shown in Figure 1, Gum Hallow Branch, Mill Branch, and Pinhook Branch represent other tributaries of significant length. As can be observed from the figure, EFPC is recharged by BC, Gum Hollow Branch, Mill Branch, and Pin Hook Branch, in addition to 30 unnamed tributaries. These tributaries were all included in the model.

Geological formations beneath ORR include primary groups recognized as: the Knox, Rome, Chickamauga, and Conasuaga, Sequatchie, Fort Payne Chert, Rockwood, Copper Ridge Dolomite, and Maynardville Limestone formations. The Knox Aquifer and

the Chickamauga Group are the dominant hydrologic units. In these leaky confining units, flow is dominated by fractures and relatively low hydraulic conductivities.

Land cover includes intensive agriculture, urban and industrial, or areas of thick forest. White oak, bottomland oak, and sycamore-ash-elm riparian forests are the common forest types in the areas. Grassland barrens intermixed with cedar-pine glades also occur here.

1.2 Modeling Applications

Modeling tools have been used extensively to simulate system dynamics. Models are generally categorized as stochastic or deterministic, and further classified as conceptual or empirical depending on their ability to obey the physical laws. Stochastic models are dependent upon random variables dominated by a probability distribution function. In deterministic models all the input parameters are known within a specific certainty range.

Studies have employed computer models to emphasize the significance of sediments and suspended matter in contaminant transport. A mass balance model was used to evaluate the internal load of mercury particulates associated with resuspension of contaminated sediment [**24**]. Models have also been used to predict mercury exposure in hypothetical piscivorous birds and mammals through fish consumption [**25**]. A study performed by the North Carolina Department of Natural Resources revealed that 75% of the total mercury load present in the Cashie River Watershed resulted from eroded sediments [**26**]. A study on the development of a mercury speciation applied to the Lohatan Reservoir in Nevada, showed that 90% of the mercury released into the system was maintained within the sediments and constituted a continuous source of pollution [**27**].

MIKE SHE and MIKE 11 software has been extensively applied in the areas of water resources engineering to model and understand complex system dynamics. For example, these modeling systems have been employed by the South Florida Water Management District in an integrated approach that successfully simulates wetland dynamics as part of the Everglades Nutrient Removal project [**28**]. The models have also been applied in Broward County to develop an Integrated Water Resources Master Management Plan [**29**]. Similarly, Cabrejo analyzed how mercury within the sediment serves as a continuous source of pollution within portions of Y-12; a sub-domain of the EFPC Watershed [**11**]. A study simulating flow and mercury transport in upper portions of EFPC also confirmed that for the sub-domain, a large portion of the mercury in the river is present as mercury bound to sediment particles [**15**]. These studies summarize the importance of the adsorption-desorption process in mercury contaminated environments, especially when the contaminant has an affinity to sorbs to soils in the sediment bed layer.

In this report, results for simulated discharges and contaminant concentration levels are presented in the form of time-series. Probability exceedance curves were developed from each set of time-series. Flow, discharge and mercury mass rate probability exceedance curves were developed for various hydrological regimes. The model was used as an investigative tool for the development of components of a mercury TMDL analysis.

2. RESEARCH OBJECTIVE

This research is a continuation of efforts to correlate the hydrology of the EFPC and BC with the long-term distribution of mercury within the overland, subsurface, river, and vadose zone sub-domains. The main objective of this thesis is to successfully integrate ECO Lab in the EFPC Watershed model as a computational mechanism for mercury exchange throughout the water column and to apply the enhanced model towards the development of TMDL analysis components. The application seeks to demonstrate the capability of the enhanced model to support efforts to understand and manage mercury contamination and remediation.

3. RESEARCH METHODOLOGY

The following approach was applied in modifying and executing the hydrology and transport model developed in support of the DOE's remediation strategies for the EFPC watershed. These techniques expand upon previous modeling efforts, including the diffusive transport between the water column and sediment pore water, and the adsorption-desorption processes between dissolved mercury and suspended matter in the water column as part of the total mercury concentration. The techniques implemented build upon the process established by the Environmental Protection Agency (EPA) for model development by considering the three main steps: (a) identification of the environmental problem the model is intended to resolve, (b) development and or evaluation of the mathematical model, and (c) parameterization of the model for viability as an applicable tool [**19**].

3.1 Approach

It is important to note that the approach in this study took advantage of the previous efforts to model the hydrological environment and mercury transport dynamics within the ORR made by Long and Cabrejo. Long created a baseline model capable of simulating the hydrology and mercury transport throughout the entire EFPC Watershed. Cabrejo focused on a sub-section of the watershed, known as UEFPC, and instead considered as factors adding to the total mercury concentration, the diffusive transport between the water column and sediment pore water and the adsorption-desorption processes between dissolved mercury and suspended matter in the water column. This research combines both methods by incorporating ECO Lab to simulate the fate and transport of mercury at the water and sediment interface throughout EFPC.

The integrated surface/sub-surface model was built using the numerical package, MIKE (MIKE 11 coupled with MIKE SHE and ECO Lab), which was developed by the Danish Hydraulic Institute (DHI). The sedimentation module originally included in the UEFPC was added and included in the entire EFPC watershed model.

The sedimentation and water quality modules were included in the EFPC watershed model in the following phases:

1. The water quality and sedimentation modules (ECO Lab) were added to BC and for the remaining section of EFPC (downstream of Station 17) to include EFK 6.4.
2. Water quality, transport, and sediment-related parameters, such as carbon partitioning coefficient, adsorption rates of mercury species to sediment particles and water molecules, resuspension rate of sediments, settling velocity of suspended particles, and critical current velocity for sediment resuspension, were estimated from the

extensive calibration exercised for the UEFPC model by previous researchers as well as DOE reports of field surveys, laboratory experiments reported by FIU or other research institutes, and referenced publications.

3. The approach implemented for the processing of ORNL data included:
    a. Data was checked for validity based on database markers and categorized into spreadsheets.
    b. New stations were added to GIS maps of the site.
    c. Time-series files were developed from field records and dynamically linked to model boundary conditions.

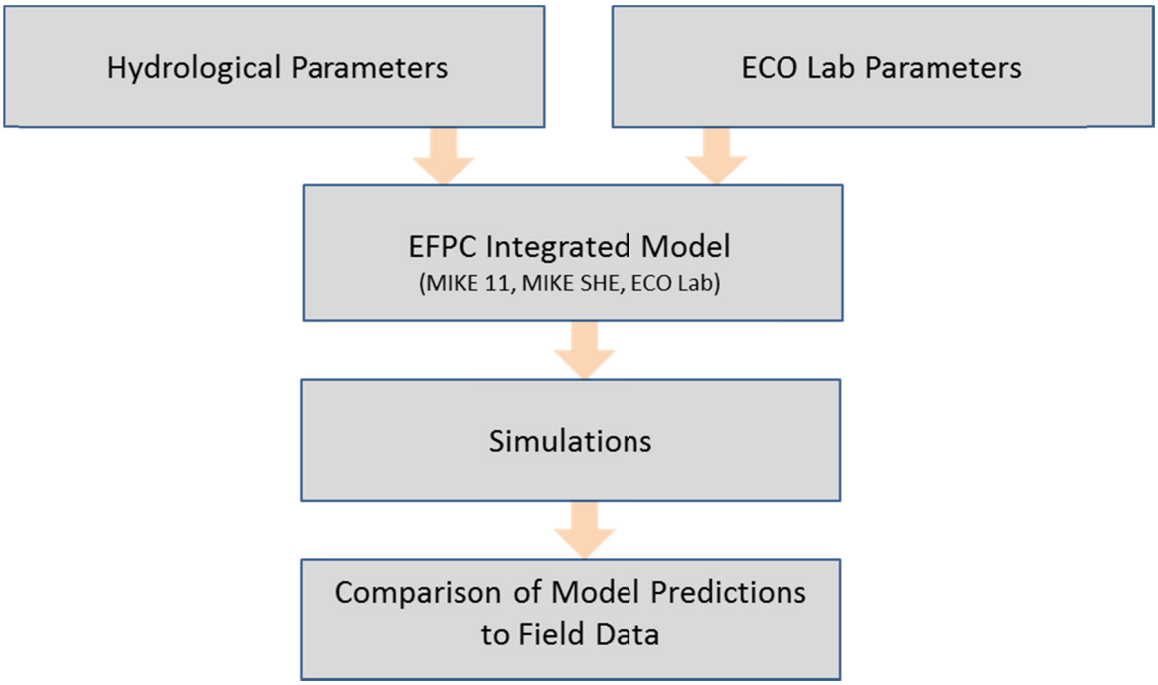

Figure 3. Procedure flow diagram for modeling the hydrology and transport using for the updated EFPC watershed model.

Model nodes, cross-sections, and boundaries were added and modified as necessary due to the addition of new observation stations and the need to reduce both numerical

instabilities and computational time. Simulations were executed to correlate stochastic hydrologic events and stream flow with mercury-distribution patterns.

This study did not include any calibration or validation for either flow or transport parameters. Instead, the study focused on the analysis of a comparison between predictions by the model, using parameters and available field data for flow at a number of field stations and for total measurements of mercury at the only monitoring station in the EFPC (i.e. Station 17).

3.2 EFPC Model Overview

The model includes the main components of the hydrological cycle and contaminant transport; groundwater flow and transport (three-dimensional saturated and unsaturated), overland flow, flow in rivers, precipitation, and evapotranspiration. The model enables full dynamic coupling of surface and subsurface flow processes, which allows calculations of water and contaminant exchange between the land, rivers, and the groundwater. By providing detailed spatial information and characteristics, including hydrological and transport properties in the four sub-domains; saturated zone, unsaturated zone, overland flow, and transport in streams, the model provides accurate water and contaminant mass balance for the domain. MIKE SHE and MIKE 11 are used to simulate and assess the impact of hydrological events on mercury contamination. The processes simulated by each module (MIKE 11, MIKE SHE, and ECO Lab) in the EFPC model are shown in Figure 4 and explained in greater detail within the subsequent sections.

Figure 5 provides a conceptual schematic based on the EFPC model modular set up. The diagram denotes the various pathways of interaction among the MIKE SHE, MIKE

11, and ECO Lab modules and lists the numerical engines associated at each level of computation. Figure 6, provides a detailed schematic of the MIKE SHE module presented in Figure 5.

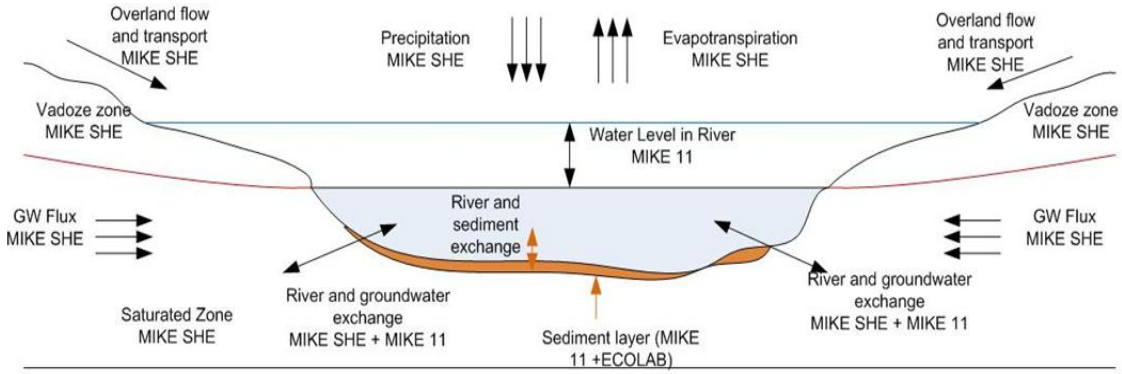

Figure 4. Processes simulated by MIKE modules [15].

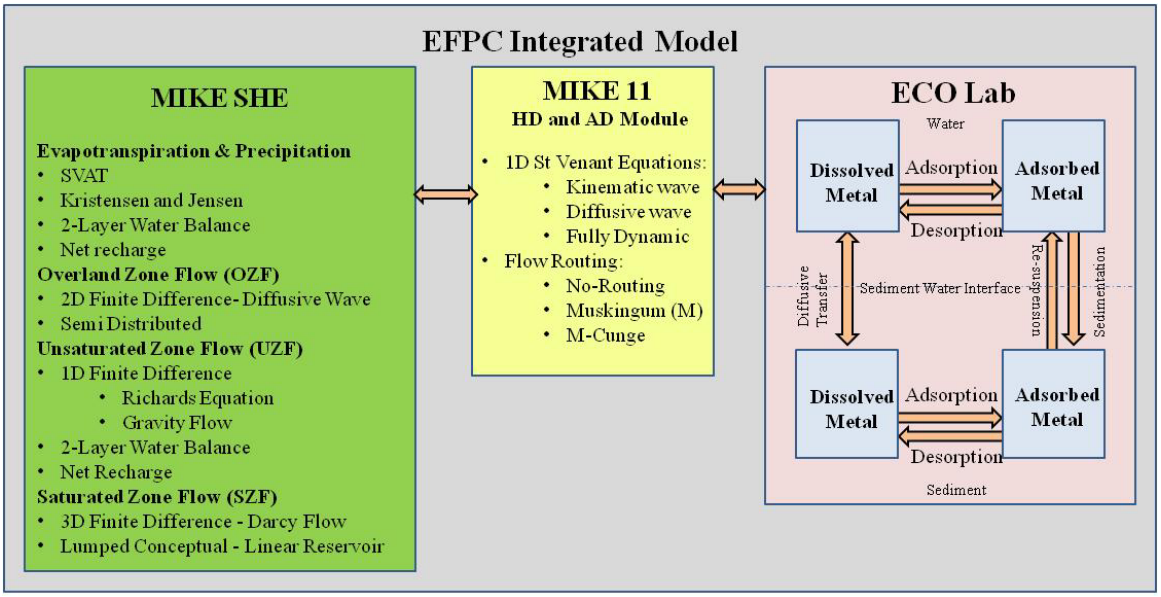

Figure 5. Schematic of the modular set-up and processes of MIKE SHE, MIKE 11, and ECO Lab arranged in accordance to the EFPC model structure (concept obtained from DHI [30] and modified by Lilian Marrero).

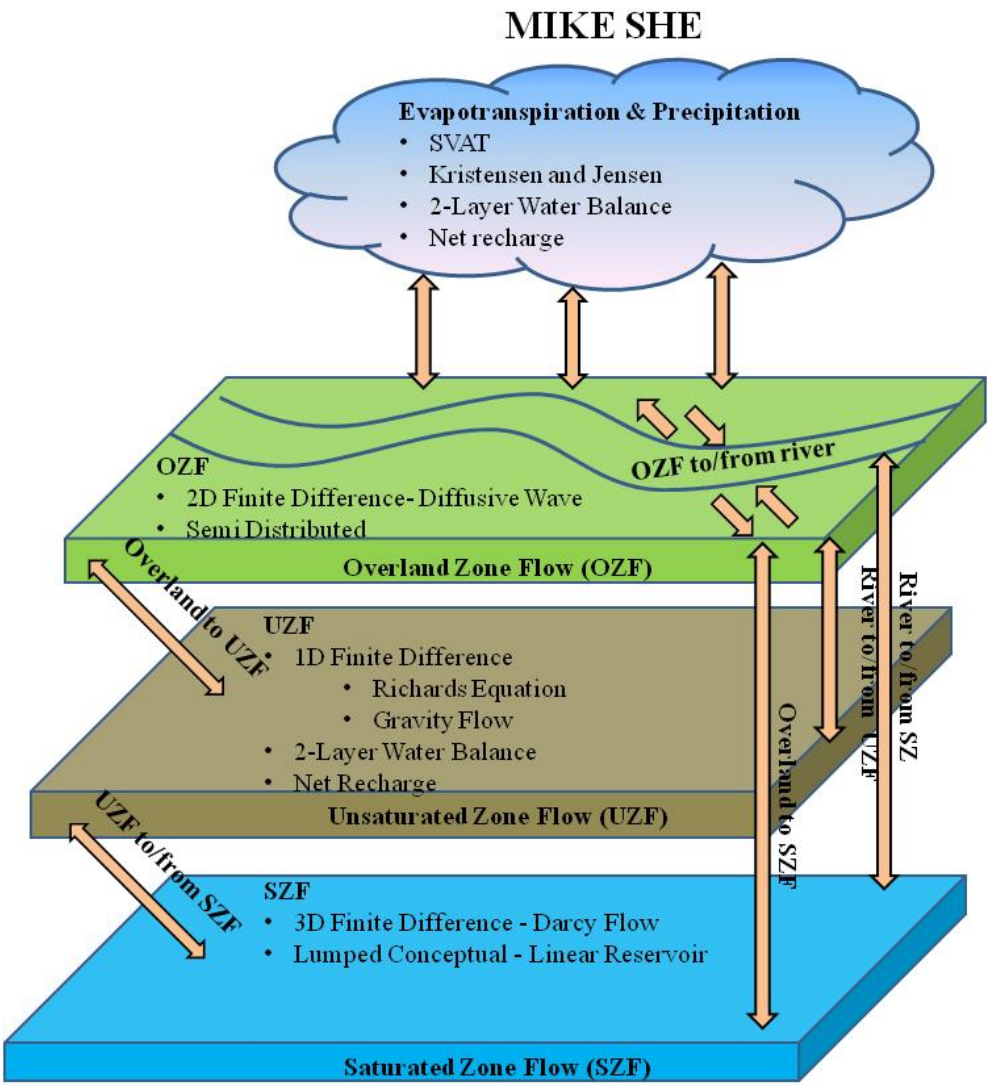

Figure 6. Detailed schematic of MIKE SHE setup and processes (concept obtained from DHI [30] and modified by Lilian Marrero).

3.2.1 MIKE 11 and MIKE SHE

MIKE 11 is a one-dimensional river flow and transport model that requires longitudinal profiles, cross-sections, Manning's numbers, and other hydrodynamic parameters [**31**]. It uses the dynamic Saint Venant equations to determine river flow and water levels. The complete nonlinear equations of open channel flow (Saint-Venant) can be solved numerically between all grid points at specified time intervals for given boundary conditions. In addition to this fully dynamic description, other descriptions are also available to choose from, including high-order, fully dynamic, diffusive wave, kinematic wave, quasi-steady state, and kinematic routing (Muskingum, Muskingum-Cunge).

MIKE SHE is a fully integrated model for the three-dimensional simulation and linkage of hydrologic systems, including overland, subsurface, and river flows. It has been successfully applied at multiple scales, using spatially distributed and continuous climate data to simulate a broad range of integrated hydrologic, hydraulic, and transport problems. MIKE SHE represents the two-dimensional overland, one-dimensional unsaturated zone, three-dimensional saturated and vadose zone flow and transport components [**30**]. The hydrologic processes are described based on physical laws, such as the conservation of mass, energy and momentum. MIKE SHE couples several partial differential equations that describe flow in the saturated and unsaturated zones with the overland and river flow. Different numerical solution schemes are then used to solve the different partial differential equations for each process. A solution to the system of equations associated with each process is found iteratively by use of different numerical solvers.

The model enables MIKE SHE and MIKE 11 hydrodynamic modules to interact through branches or stream reaches defined within the domain. This coupling allows for the one-dimensional simulation of river flows and water levels through the fully dynamic Saint Venant equations. Hydraulic control structures, area-inundation modeling, dynamic overland flooding flow in relation to the MIKE 11 river network, and the dynamic coupling of surface and sub-surface flow is simulated. Floodplain flooding is simulated by first establishing the floodplain through the MIKE SHE topography and then activating the direct overbank spilling option in MIKE 11 while simultaneously restricting cross-sections to the main channel. The cross-sections defined in MIKE 11 are used to calculate the river water levels and volumes. Consistency with topographical elevations is of extreme importance since the bank elevation is the primary reference for cell flooding. River and groundwater exchange is modeled by defining the river in contact with the aquifer. In this case, the water exchange between MIKE 11 and MIKE SHE is performed through a river-link cross section. The river cross-sections link is a function of conductance, the grid node, and river linkage.

3.2.2 ECO Lab

The concept of mercury transport through stream sediments or total mercury load and the water column is compartamentalized into bed load, suspended load, and dissolved load [**32**]. ECO Lab is an equation solver; applied in this case to handle the sedimentation and exchange of mercury within sediments, suspended particles, pore water and dissolved mercury species [**33**]. An ECO Lab template can be developed by the user to model the ecological processes as required by any specific project; however, some templates have already been developed by DHI in the areas of water quality (17

templates), heavy metal transport (1 template), eutrophication (3 templates), and xenobiotics (1 template). For the modeling of mercury fate and transport in EFPC, the heavy metal transport template of ECO Lab is used coupled with both MIKE 11 and MIKE SHE to simulate the interaction of mercury species with the sediment particles and water molecules in the creek. The heavy metal template describes the adsorption/desorption of mercury to suspended matter, the sedimentation of sorbed mercury to the streambed, as well as resuspension of the settled mercury. It also includes exchange of mercury between particulates of the bed sediment and the interstitial waters of the bed. The diffusive exchange of dissolved mercury in the water and in the interstitial waters is also considered.

3.3 Model Theory

The basic theory behind the EFPC Watershed model is discussed in the following sub-sections for the various modules included; such as, MIKE SHE, MIKE 11, and ECO Lab.

3.3.1 MIKE SHE

Saturated, unsaturated, and overland flows are some of the central processes accounted for through the MIKE SHE module. The theory behind the MIKE SHE module is summarized in this section and discussed in greater detail within the DHI MIKE SHE user manual [**30**].

Overland flow is computed using the diffusive wave approximation of the Saint Venant equations. The diffusive wave approximation does not account for momentum losses due to local and convective acceleration and lateral inflows [**30**], yet reduces the

complexity of the numerical solution. The simplified diffusive wave approximation solution is summarized in the equations below.

$$S_{fx} = -\frac{\partial h}{\partial x}\left(z_g + h\right) = -\frac{\partial z}{\partial x} \quad \text{(Equation 1)}$$

$$S_{fy} = -\frac{\partial h}{\partial y}\left(z_g + h\right) = -\frac{\partial z}{\partial y} \quad \text{(Equation 2)}$$

The ground surface elevation, flow depth above ground, and the friction slopes in the x and y direction are given by the variables Z, h, S_{fx} and S_{fy} respectively. These roughness coefficients are based on the Stickler/Manning law.

$$S_{fx} = -\frac{u^2}{Kx^2 h^{\frac{4}{3}}} \quad \text{(Equation 3)}$$

$$S_{fy} = -\frac{v^2}{Ky^2 h^{\frac{4}{3}}} \quad \text{(Equation 4)}$$

The discharge per unit length for the x and y direction along the cell boundary is generated by multiplying both sides of the equations by the flow depth. Per the MIKE SHE manual, this relationship between the velocities (*u* along x-direction and *v* along y-direction) and depth is given as:

$$uh = -(Kx)\left(\frac{\partial z}{\partial x}\right)^{\frac{1}{2}} h^{\frac{5}{3}} \quad \text{(Equation 5)}$$

$$vh = -(Ky)\left(\frac{\partial z}{\partial y}\right)^{\frac{1}{2}} h^{\frac{5}{3}} \quad \text{(Equation 6)}$$

The discharge per unit length is represented by *uv* along x-direction and *vh* along y-direction. The finite difference form for the velocity terms are derived in the equations

below where the north, south, east and west notations are associated with boundaries along a computational cell [**30**]. For example, the volume flow across the northern boundary is given by vh_{north}. The flow into a computational cell is the sum of all flows entering the cell from the north, south, east and west.

$$\frac{\partial(uh)}{\partial x} = \frac{(uh)_{east} - (uh)_{west}}{\Delta x} \qquad \text{(Equation 7)}$$

$$\frac{\partial(vh)}{\partial y} = \frac{(vh)_{north} - (vh)_{south}}{\Delta y} \qquad \text{(Equation 8)}$$

MIKE SHE calculates three-dimensional flow in the saturated zone through equation 9. The hydraulic conductivity (K) is considered along the x, y, and z direction. The hydraulic head, sources, and specific storage coefficients are represented by the variables h, Q, and S respectively.

$$\frac{\partial}{\partial x}\left(K_{xx}\frac{\partial h}{\partial x}\right) + \frac{\partial}{\partial y}\left(K_{yy}\frac{\partial h}{\partial y}\right) + \frac{\partial}{\partial z}\left(K_{zz}\frac{\partial h}{\partial z}\right) - Q = S\frac{\partial h}{\partial t} \qquad \text{(Equation 9)}$$

MIKE SHE computes the unsaturated flow vertically in one-dimension via the full Richards equation, a gravity procedure, or a two layer water balance method [**30**]. The full Richards equation was selected as the computing mechanism for unsaturated flow because it is the most accurate method when considering a dynamic unsaturated flow. The vertical hydraulic head (*h)* gradient shown in equation 10 includes a gravitational component and a pressure component essential for the vertical transport of water. The volumetric flow is computed using Darcy's law as shown in equation 11 and the principle of continuity is included via equation 12.

$$\Delta h = \frac{\partial h}{\partial z} \qquad \text{(Equation 10)}$$

$$q = -K(\theta)\frac{\partial h}{\partial z} \qquad \text{(Equation 11)}$$

$$\frac{\partial \theta}{\partial t} = -\frac{\partial q}{\partial z} - S(z) \qquad \text{(Equation 12)}$$

Equation 13 below, results from combining equation 10 through 12. Equation 13 applies to homogeneous and heterogeneous profiles [**30**]. This equation accounts for the hydraulic conductivity function $\left(K(\theta)\right)$ and the soil moisture retention curve $(\partial\psi(\theta))$.

$$\frac{\partial \theta}{\partial t} = \frac{\partial}{\partial z}\left(K(\theta)\frac{\partial \psi}{\partial} \right) + \frac{\partial K(\theta)}{\partial z} - S(z) \qquad \text{(Equation 13)}$$

When the concept of soil water capacity shown in equation 14 is introduced, equation 13 transforms into the Richards' equation shown in this text as equation 15.

$$C = \frac{\partial \theta}{\partial \psi} \qquad \text{(Equation 14)}$$

$$C\frac{\partial \psi}{\partial t} = \frac{\partial}{\partial z}\left(K(\theta)\frac{\partial \psi}{\partial z} \right) + \frac{\partial K(\theta)}{\partial z} - S \qquad \text{(Equation 15)}$$

3.3.2 MIKE 11

The one-dimensional numerical engine used to compute flow within the hydrodynamic module employs the Saint Venant Equations under various assumptions. The model disregards variations in density within the flow medium (water) [**31**]. Flow within rivers or streams are assumed to be parallel to the reach bottom [**31**]. Moreover, water movement perpendicular to the flow direction of the stream is disregarded [**31**].

These simplifications lead to the modified Saint Venant equations shown below; constituting the numerical foundation of the hydrodynamic module.

$$\frac{\partial q}{\partial x} + \frac{\partial A_{fl}}{\partial t} = q_{in} \qquad \text{(Equation 16)}$$

$$\frac{\partial q}{\partial x} + \frac{\partial\left(\alpha \frac{\partial q^2}{A_{fl}}\right)}{\partial x} + gA_{fl}\frac{\partial h}{\partial x} + gA_{fl}A_1 = \frac{f}{\rho_w} \qquad \text{(Equation 17)}$$

The continuity equation; shown first above, emphasizes the conservation of mass within stream sections. The second equation expresses the conservation of momentum. The variables q, A_{fl}, q_{in}, h, α, f, and ρ_w respectively represent the discharge, cross-sectional area, lateral inflow per unit length, water level, the momentum distribution coefficient, friction slope, and water density [**31**].

3.3.3 ECO Lab

ECO Lab was incorporated into the model through the advection module. The set of transport equations governing the advective ECO Lab dynamics are shown below in their non-conservative form [**33**]:

$$\frac{\partial c}{\partial t} + C\frac{\partial c}{\partial x} + v\frac{\partial c}{\partial y} + w\frac{\partial c}{\partial z} = D_x\frac{\partial^2 c}{\partial z^2} + D_y\frac{\partial^2 c}{\partial z^2} + D_z\frac{\partial^2 c}{\partial z^2} + S_c + P_c \qquad \text{(Equation 18)}$$

The ECO Lab state variables c, S_c, and P_c represent concentration, sources and sinks, and ECO Lab processes. The flow velocity components in the x, y, and z-direction are represented by *u, v,* and *w*. Similarly, the dispersion coefficients in the x, y, and z-direction are represented by D_x, D_y, and D_z. The transport equation is modified as:

$$\frac{\partial c}{\partial t} = AD_c + P_c$$ (Equation 19)

The rate of change in concentration as a byproduct of advection dispersion is accounted by the term AD_c. Per DHI, the ECO Lab solver calculates the concentration at each time step through an explicit time-integration where AD_c is constant at each time step [**33**]. The ECO Lab module is capable of performing the explicit time-integration using various methods. These methods include the Euler, Runge Kutta 4, and Runge Kutta with quality check [**33**].

$$y_{n+1} = y_n + h \cdot f(x_n, y_n)$$ (Equation 20)

$$k_1 = h \cdot f(x_n, y_n)$$ (Equation 21)

$$k_2 = h \cdot f\left(x_n + \frac{h}{2}, y_n + \frac{k_1}{2}\right)$$ (Equation 22)

$$k_3 = h \cdot f\left(x_n + \frac{h}{2}, y_n + \frac{k_2}{2}\right)$$ (Equation 23)

$$k_4 = h \cdot f(x_n + h, y_n + k_3)$$ (Equation 24)

$$y_{n+1} = y_n + \frac{k_1}{6} + \frac{k_2}{3} + \frac{k_3}{3} + \frac{k_4}{6} - O(h^5)$$ (Equation 25)

The newly added ECO Lab module within EFPC was set to perform the explicit-time integration using the Runge Kutta 4th order. This method was selected from the available previously described options because it has higher accuracy than the rest. As illustrated within the scientific manual the function in equation 20 is solved in the four steps shown

by equation 21 through equation 24. The solution y is obtained from x_n to x_{n+1} and equivalent to x_{n+h} as shown in equation 25.

In addition to the internal computational processes described, mercury transport processes in ECO Lab are defined by specifying the following [**33**]:

- Dissolved mercury concentration in the water (S_{HM}).
- Adsorbed mercury concentration on suspended matter (X_{HM}).
- Dissolved mercury concentration in the sediment pore water (S_{HMS}).
- Adsorbed mercury concentration in the sediment (X_{HMS}).

The byproduct of mercury exchange between suspended solids and the water column is represented by variable S_{HM}. This exchange is mainly driven by the organic carbon partitioning coefficient (K_d), indicating the contaminant's affinity towards the soil phase. Dissolved mercury is computed using the following set of interconnected equations [**33**]:

$$\frac{dS_{HM}}{dt} = -adss + dess + difv \qquad \text{(Equation 26)}$$

$$adss = k_w K_d S_{HM} TSS \qquad \text{(Equation 27)}$$

$$dess = k_w X_{HM} \qquad \text{(Equation 28)}$$

$$difv = \frac{f_{biot(difw)}\left(\frac{S_{HMS}}{(pors)(dzds)} - S_{HMS}\right)}{(dzwf + dzds)dz} \qquad \text{(Equation 29)}$$

The equations above clearly represent the relation between adsorption ($adss$), desorption (*dess*), and diffusive transfer (*difv*). The variables k_w, K_d, TSS, $f_{biot(difw)}$, *pors*, *dzwf* and *dz* are equivalent to the desorption rate (d^{-1}), partitioning coefficient for

mercury (m^3 H_2O/gDW), total suspended solids concentration (g DW/m^3 bulk), the dimensionless factor for diffusion due to bioturbation, thickness of diffusion layer in sediment, and thickness of the computational grid layer respectively.

The adsorbed mercury concentration on suspended matter within the water column X_{HM} results from mercury being absorbed by both the suspended solids and particles resuspended by the river bed layer, and eliminating the mercury desorbed from suspended solids into water column, and also those adsorbed by settling particles.

$$\frac{dX_{HM}}{dt} = adss - dess - sev + resv \quad \text{(Equation 30)}$$

$$sev = \frac{v_s X_{HM}}{dz} \quad \text{(Equation 31)}$$

$$resv = \frac{RR\frac{X_{HMS}}{X_{SED}}}{dz} \quad \text{(Equation 32)}$$

In the equations above, the variables *sev* and *resv* represent the sedimentation and resuspension of particles. The settling velocity (m/d) of suspended solids is defined by v_s . The resuspension rate is denoted by the variable *RR* (gDW/m^2/d). Meanwhile, the sediment mass is represented by X_{SED} (gDW/m^2). These equations assume that the current speed is greater than the critical speed responsible for initiating movement [**33**]. S_{HMS} is calculated based on the equations below:

$$\frac{dS_{HMS}}{dt} = -adss + dess - dif \quad \text{(Equation 33)}$$

$$adss = k_s K_{ds} S_{HMS} \frac{X_{SED}}{dzs \cdot por_s}$$ (Equation 34)

$$dess = k_s X_{HMS}$$ (Equation 35)

The desorption rate in sediment (d^{-1}), metal partitioning coefficient between particulates and water (m^3 H_2O/gDW), and sediment porosity (m^3 H_2O/ m^3 bulk), are given by k_s, K_{ds}, and por_s. The variables in the above equations have been defined earlier in this section.

X_{HMS} is calculated using the following:

$$\frac{dX_{HMS}}{dt} = adss - dess - sev + resv$$ (Equation 36)

$$adss = k_s K_{ds} S_{HMS} \frac{X_{SED}}{dzs \cdot por_s}$$ (Equation 37)

$$sev = v_s X_{HM}$$ (Equation 38)

$$resv = \frac{RRX_{HMS}}{X_{SED}}$$ (Equation 39)

4. MODEL ENHANCEMENT AND APPLICATION

The EFPC model originally developed by Long has been extended and improved throughout the course of this study as summarized in Figure 7. The model has been extended to include observation stations not previously considered within the MIKE SHE module. This was performed upon evaluating the most recent publicly available historical data for the site. Internal numerical parameters within the simulation specifications were evaluated and updated to decrease the computational time within the model's pre-processing, water movement, and water quality computational phases. In addition, data was reformatted to increase pre-processing speed. For example, vegetation data input format was changed from shape to gridded codes.

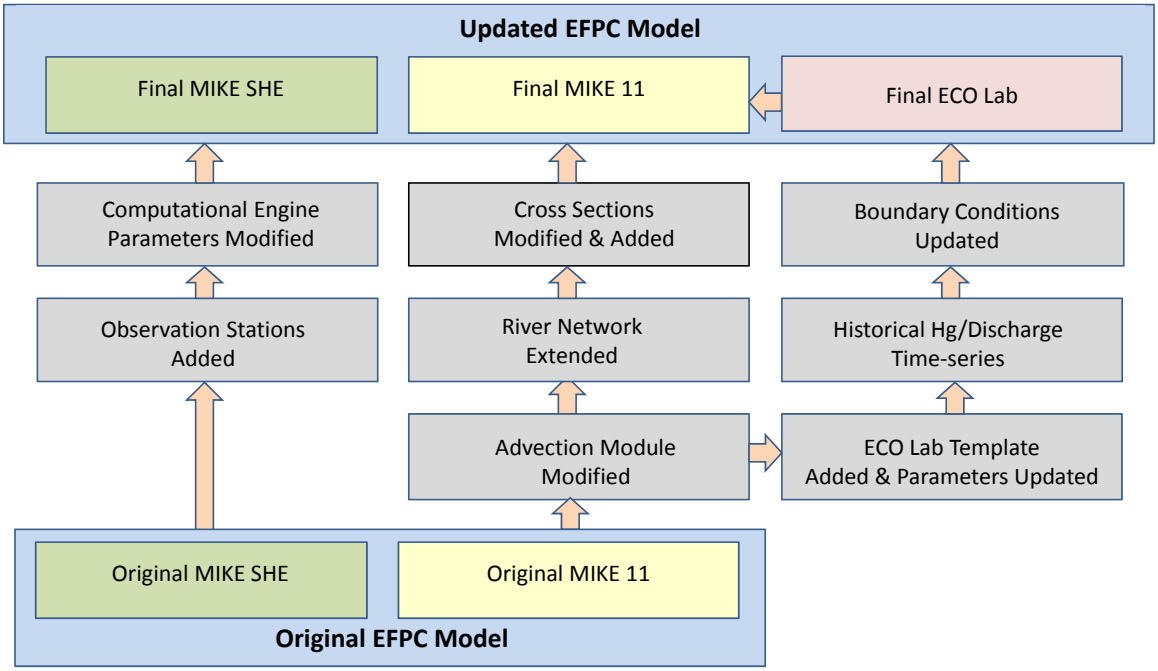

Figure 7. Changes and enhancements made to EFPC model.

The MIKE 11 component of the model also underwent various transformations. The advection module was modified to include ECO Lab, the watershed river network was extended significantly when compared to the baseline EFPC Watershed model, and cross-

sections were added to reduce flooding at points of high numerical instabilities. Existing river cross-sections were also examined and altered to ensure consistency in bed level elevations at the branch junctions and thus reduce numerical instabilities. Furthermore, the newly incorporated ECO Lab template was adjusted to include state variables, forcings, values, and constants previously defined for the localized Y-12 model. The following sections provide an overview of changes implemented to the baseline model.

4.1 Data Extraction and Processing

The Oak Ridge Environmental Information System (OREIS) is a centralized, standardized, quality-assured, and configuration-controlled environmental data management system belonging to the DOE. The environmental data retrieved from the OREIS database for the purposes of this research include known quality measurement and spatial data for groundwater, surface water, sediment, and soil. The spatial data was extracted by utilizing the OREIS spatial query tool, Figure 8 (A).

During the data extraction process, the domain was divided into 16 sub segments in an effort to minimize the time and computer resources spent in the data extraction process. The data was initially extracted in the form text files. It was archived into spreadsheets, converted into appropriate units, formatted as time-series, and added to the model as additional observation stations. Stations 2236AQ06, 3538250, 3215AQ05, 3904AQ04, EFK 13.8, 5313AQ03, EFK 18.2, 6262AQ02, and 6361AQ01 shown in Figure 38 were initially identified as potential observation stations to be added to the model.

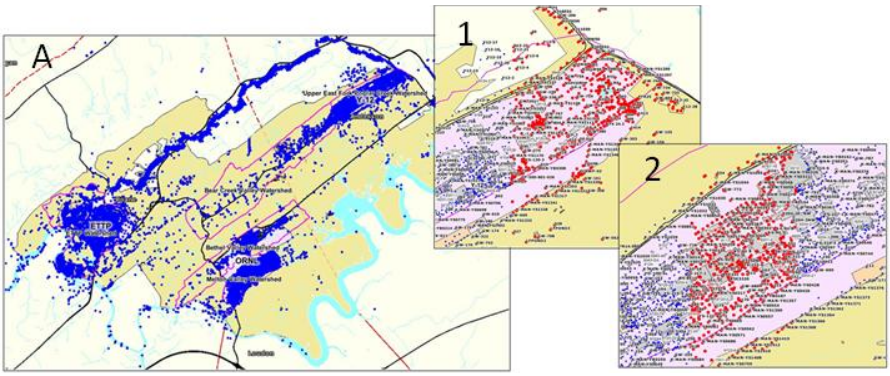

Figure 8. OREIS spatial query tool (A), and sample segments extracted (1) - (2).

Additional stations considered but discarded based on the invalid declaration of the OREIS validation qualifier include PCM 5.5-1, PCM 5.5-2, PCM 5.5-3, PCM 5.5-4, PCM 5.5-5, PCM 6.0, PCM 6.5, PCM 7.0, LASD01, and CCSD01. Ultimately, 3538250, EFK 13.8, and EFK 18.2 were the only new discharge (flow rates measurements) stations with sufficient data to be included in the model. The relative location of both processed field stations and stations added to the model is shown in Figure 38. Specific coordinates are maintained confidential.

4.2 Model Domain, Topography

The study area is contained within the red outline in Figure 9. GIS files for the domain, USGS observation stations, streams, water bodies such as lakes, and topography were inserted into the model in the form of either shape files or MIKE Zero shell extensions (dfs0, dfs1, or dfs1). Figure 9 (A) shows an overlay of these files as it appears within the model's display section. Surface elevations were originally embedded in the model in the form of a dfs2 extension file. These surface elevations are measured in meters. Figure 9 (B), (C), and (D), show GIS shape files for soil imperviousness, soil type and land use. These files were introduced in MIKE SHE and prepared by previous members of the Applied Research Center (ARC) - Environment and Water Resources

Group during the initial stages of model development. Refer to Long [**23**] for a more detailed explanation of their assembly.

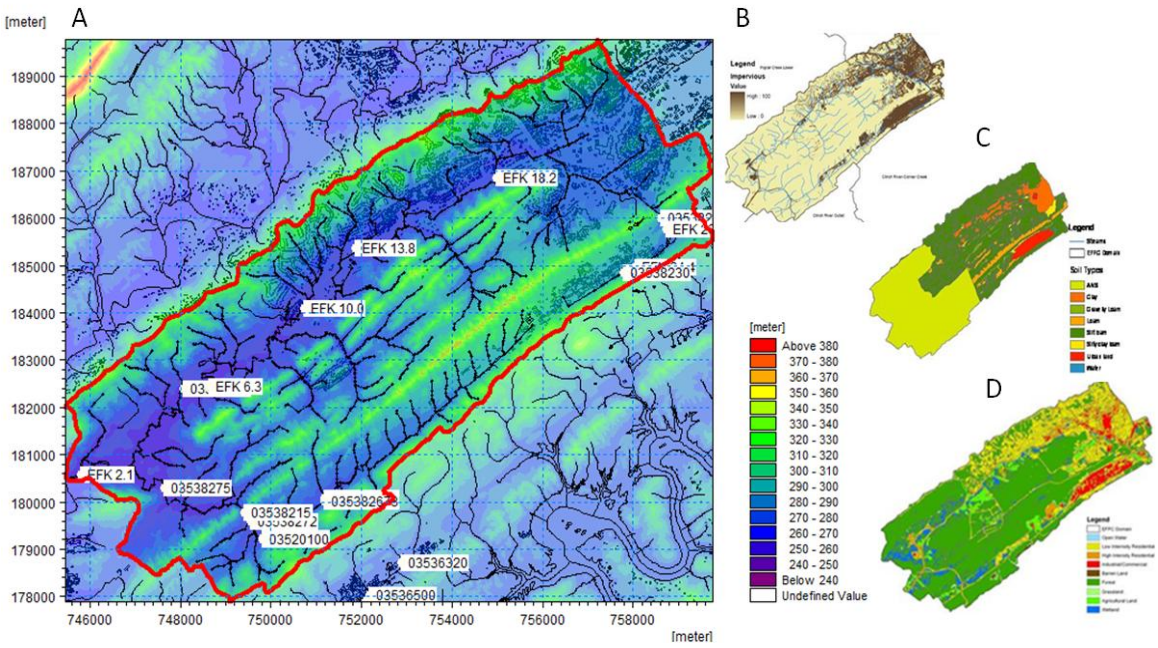

Figure 9. Image overlay of observation stations, streams, water bodies, and topography (A), imperviousness (B), soil type (C), and land use (D) (obtained from Long and Malek-Mohammadi, modified by Lilian Marrero [15] [23]).

4.3 Climate

Hydrological climate patterns such as precipitation, snowmelt and evapotranspiration, form part of the climate sub-section within MIKE SHE. The precipitation component of the model determines surface water flows and defines the basics for the groundwater table. The precipitation time-series is presented as a rate in the form of mm/day from 1/1/1950 through 12/31/2008. The MIKE SHE module will only use the precipitation data within the user-specified time period. It must be noted that snow melt is not included as a sub-component of the climate since the precipitation values reported in the time-series already account for frozen precipitation.

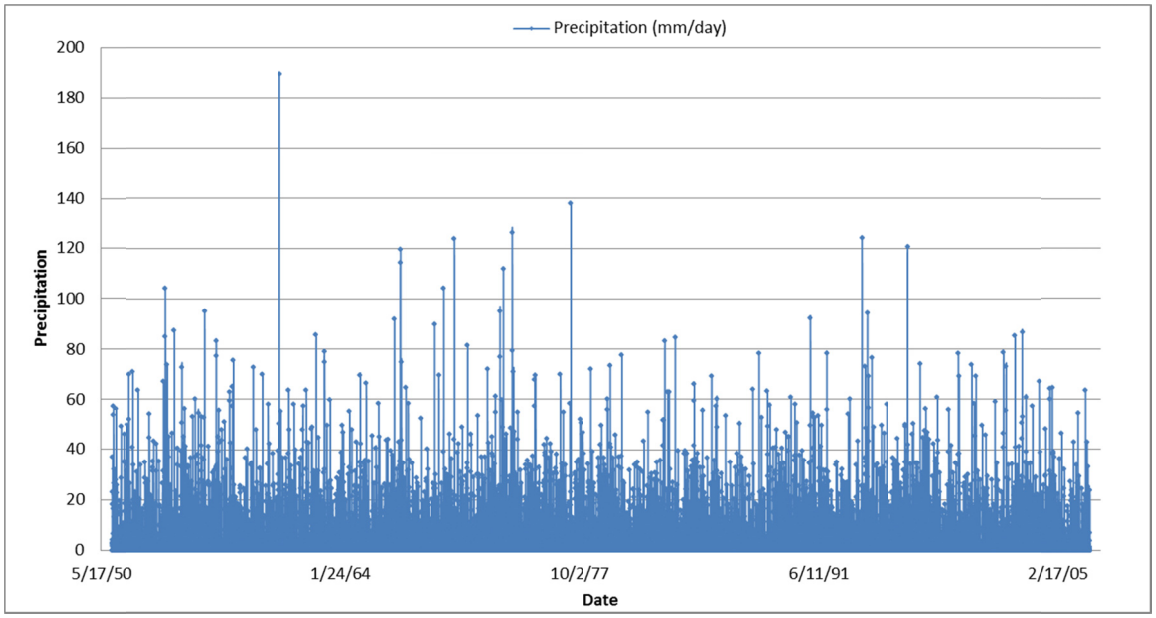

Figure 10. Precipitation time-series data from January 1, 1950 through December 31, 2008.

The evapotranspiration component of the model is dependent upon meteorological and vegetative data as it must predict evapotranspiration due to rainfall interception by canopy, canopy drainage to soil surface, evaporation from plant and soil surface, and water uptake by roots. A spatially uniform constant value of 2.01168 mm/day is observed based on records for the state of Tennessee [**23**]. The model adjusts evapotranspiration based on the leaf area index and root depth specified under land use.

4.4 Land Use

The land use consists of vegetation maps with assigned leaf area index constants and root depth values obtained from USGS. These parameters spatially adjust the reference evapotranspiration stated previously. The table below depicts the gridded codes and their classification along with assigned leaf area, root depth and Manning's M (defined the inverse of Manning's roughness coefficient).

Table 2. Land usage classifications.

Grid Code	Class	Leaf Area Index	Root Depth (mm)	Manning's M (1/n)
11	Open water	0	0	50
21	Developed, Open Space	3	2000	50
22	Developed, Low Intensity	2.5	2000	20
23	Developed, Medium Intensity	2	2000	10
24	Developed, High Intensity	1.5	2000	7
31	Barren Land, Rock, Sand, Clay	1.31	4000	11
41	Deciduous Forest	5.5	2000	10
42	Evergreen Forest	5.5	1800	9
43	Mixed Forest	5.5	2400	10
52	Shrub, Scrub	2.08	2500	20
71	Grassland, Herbaceous	1.71	1500	29
81	Pasture, Hay	1.71	1500	30
82	Cultivated Crops	3.62	1500	27
90	Woody Wetlands	6.34	2000	10
95	Emergent Herbaceous Wetlands	6.34	2400	22

4.5 Saturated Zone

The saturated zone includes subsurface drainage where the distribution of hydrogeologic parameters is assigned via geological layers [**31**]. A layer from 0 meters to 30 meters below ground level and another from 30 to 100 meters below ground surface were added to the model. This generalizes a two-layer aquifer profile for the site. Parameters influencing saturated flow are considered in this section. A horizontal hydraulic conductivity, vertical hydraulic conductivity, specific yield, and specific storage of 1.0 e^{-04} (m/s), 1.0 e^{-05} (m/s), 0.2 (dimensionless) and 3.0 $x10^{-5}$ (m^{-1})formed part of the original model and remain unchanged in the current version. The drainage level was assumed -1.0 m relative to the ground, and the drainage time constant has been preset to $1.0x10^{-6}$ sec^{-1} based on calibration and uncertainty analysis performed by previous modelers.

4.6 Unsaturated Zone

The unsaturated zone employs the Van Genuchten's algorithm in the computation of hydraulic conductivity and water retention curve ; where the water content $\theta(\psi)$ is a function of tension ψ [**30**]. The relationship between the two is based on defined parameters and summarized by the equations that follow [**30**]:

$$\theta(\psi) = \theta_r + \frac{(\theta_s - \theta_r)}{[1 + (\alpha\psi)^n]^m} \qquad \text{(Equation 40)}$$

$$m = 1 - 1/n \qquad \text{(Equation 41)}$$

$$K(\psi) = K_s \frac{\left(\left(1 + |\alpha\psi|^n\right) - |\alpha\psi|^{n-1}\right)^2}{\left(1 + |\alpha\psi|^n\right)^{m(l+2)}} \qquad \text{(Equation 42)}$$

Table 3. Upper and lower aquifer retention curve parameters.

Hydraulic Conductivity Curve Parameters									
Upper Layer					Lower Layer				
K_s	α	n	Shape factor	m	K_s	α	n	Shape factor	m
4.05e-5	0.124	2.28	0.5	0.5614	1.95e-7	0.01	1.23	0.5	0.1869

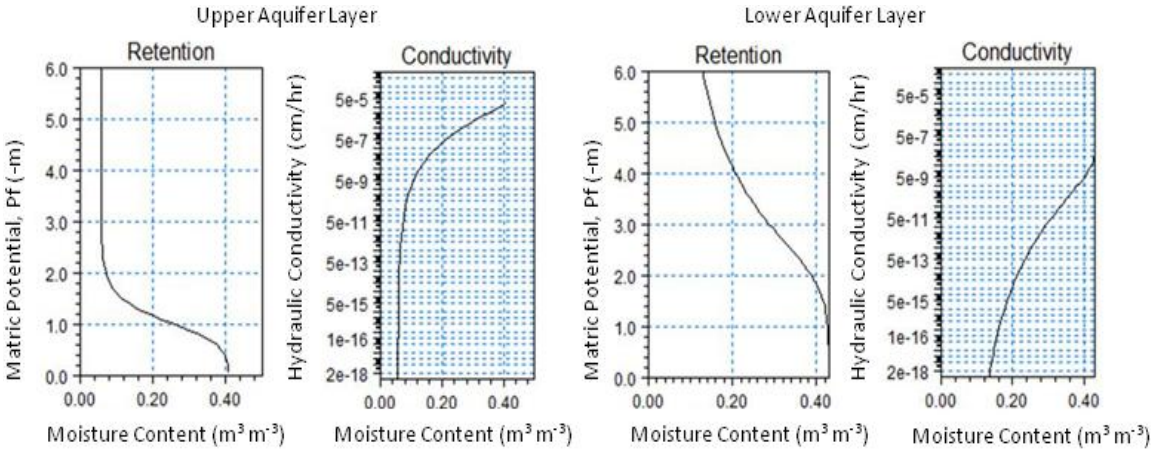

Figure 11. Retention and hydraulic conductivity curves for the upper and lower aquifer layers.

The saturated moisture content (θ_s), residual moisture content (θ_r), the α-empirical constant inversely related to air entry, and the m and n-empirical constant must be specified in order for the algorithm to function. These parameters are summarized in Table 3. The retention and conductivity curves are shown in Figure 11.

The hydraulic conductivity function ($K(\psi)$) is expressed as a ratio between the hydraulic conductivity for given water content and the saturated hydraulic conductivity (K_s). Input parameters for the equations were obtained from literature for the upper and lower aquifer hydraulic conductivity and moisture retention curves.

4.7 Overland Flow

Drainage in the overland zone is routed downhill based on adjacent drain levels. If drain flow is produced it is routed to the recipient point using a linear reservoir routing technique based on a pre-processor generated reference system that utilizes the slope of the drains calculated from the drainage levels in each cell.

4.8 Channel/River Flow

Water flow is simulated in MIKE 11 via a one-dimensional engine directly linked to the network geometry [**31**]. The network developed for the EFPC model consists of reaches, nodes, grid points, and cross-sections. The river and stream network for the domain area is shown below. It consists of 112 branches or MIKE SHE links, and 1086 nodes. Separation of nodes is done in accordance with the minimum requirements of the model for numerical analysis. Nodes placement was determined based on the variation of cross-section of the creeks as a function of topography, ground characteristics, and geometry. Nodes were also added at locations exhibiting numerical instabilities due to drastic variations in the longitudinal slope.

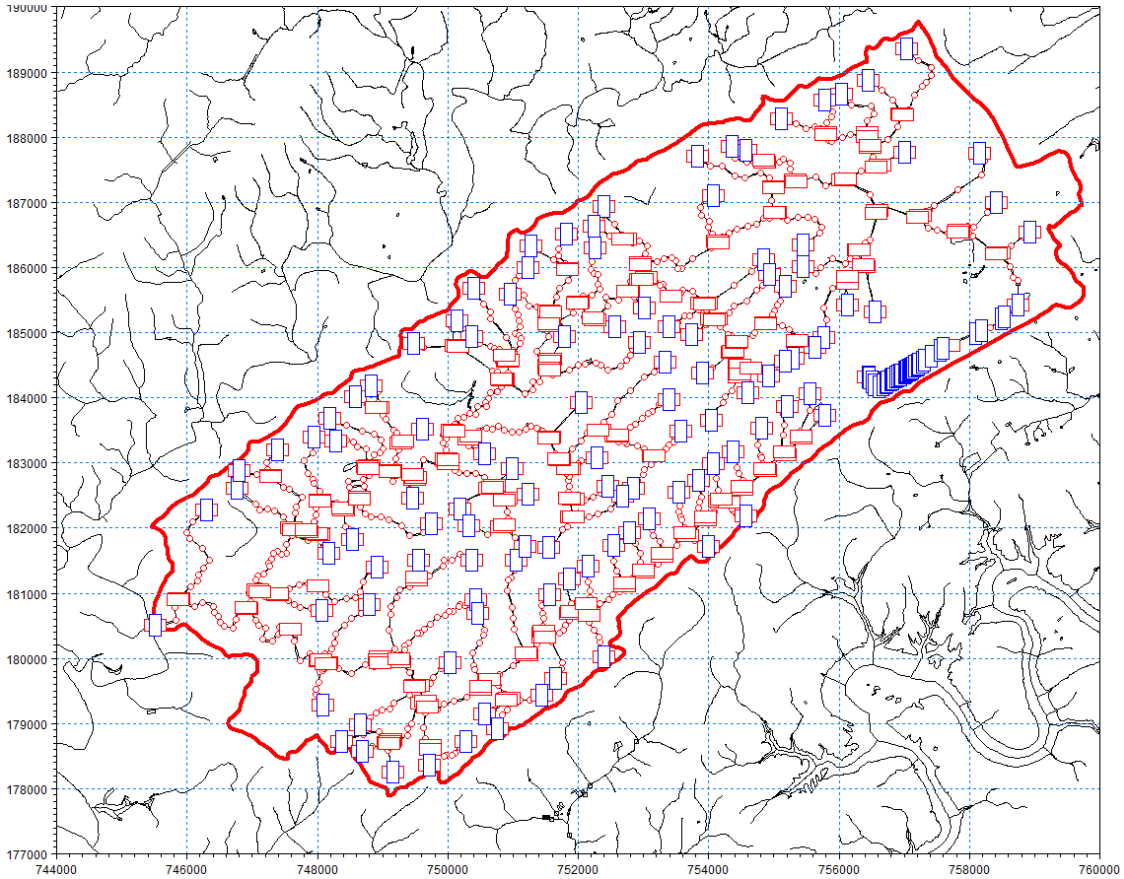

Figure 12. River network with point nodes, boundary conditions and cross-sections.

4.8.1 Boundary Conditions

The watershed model has well defined boundary conditions. The boundary conditions guide the interaction between the model domain and the surrounding external areas [**30**] [**31**]. Open boundary conditions were paired with additional boundary point sources to simulate the hydrology of the natural environment as well as the most significant anthropological alterations to the site.

The EFPC model was modified by adding outfalls (point sources) to the boundary file in both the hydrodynamic and advection module. The newly developed boundary conditions file for the modules consist of a merger between the previously existing EFPC Model boundary file and the Y-12 Model. The new boundary condition file consists of a

total of 157 branches of which 42 were declared point sources. These point sources listed in the Appendices includes discharge and mercury time-series for the hydrodynamic and advection modules.

4.8.2 Cross-Sections

The cross-sections are a two-dimensional intersection of the stream [**31**]. These are perpendicular to the stream direction. As described within the MIKE 11 user manual, the geometry of the cross-section defines the volume of water for a specific water level at the cross-section. Alternatively, the user-specified resistance defines the easiness of flow through the stream.

The original EFPC model had numerical instabilities within the MIKE 11 module as the water depth within the original set of cross-sections was routinely exceeding the allowable cross-sections depth. These numerical instabilities were eliminated by adding cross-sections to network segments that exhibited drastic slope variations. Cross-sections were generated for EFPC using a raw data approach requiring left and right bank elevations along with bed elevations. The raw data is automatically processed within the model during simulations. Storage width, flow area, resistance number, and hydraulic radius values are generated for each cross-section during the pre-processing stages of the simulation. The final network file used in simulations is shown in Figure 13, and reveals all the model cross-sections included within the domain. All cross-sections were checked for consistency in the left and right bank elevations, and bed layer elevation against available topography elevation maps for the site. Furthermore, overbank spilling was allowed in all cross-sections.

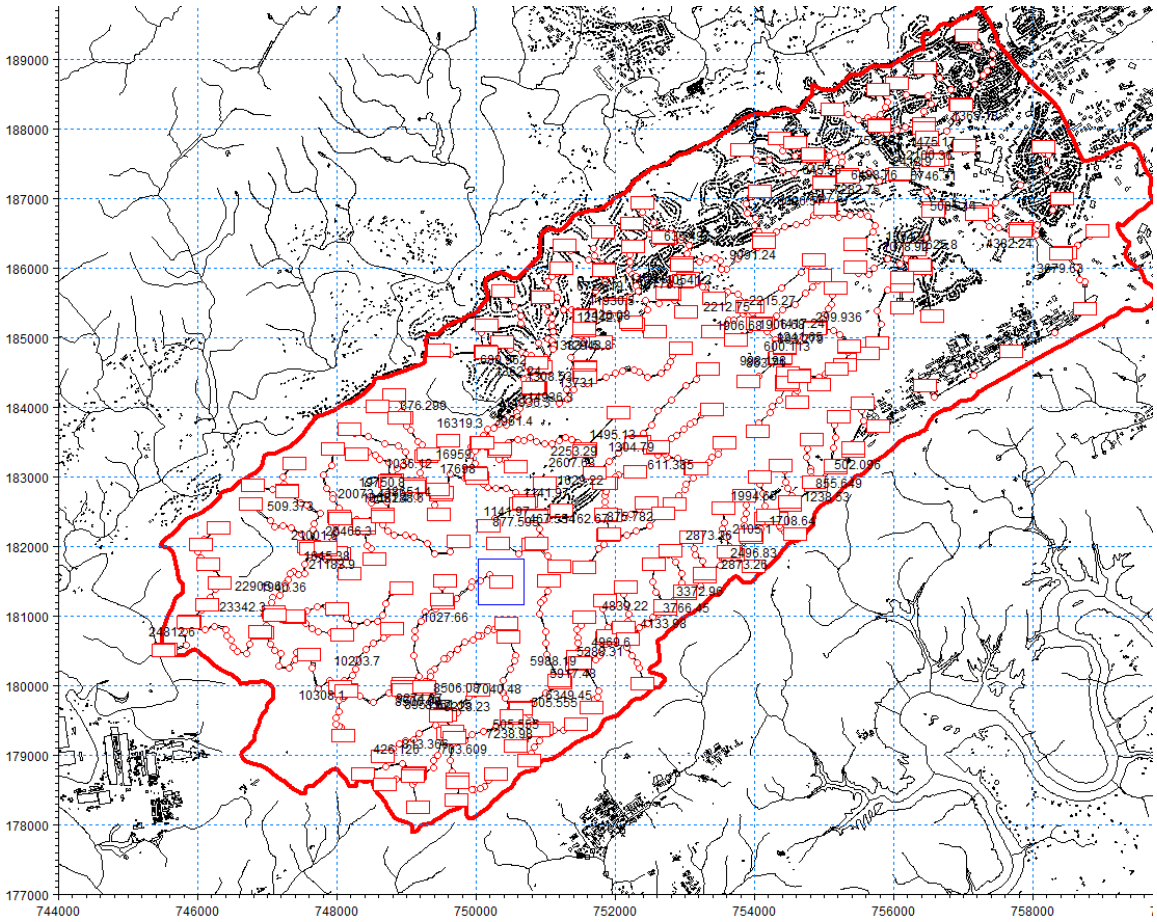

Figure 13. Overview of all river cross-sections in the model.

River cross-sections within the model were generalized as trapezoidal. Resistance (inverse of Manning's n) values range between 10 and 20 throughout the domain. A model snapshot depicting a detailed schematic of a river cross-section for EFPC is shown at chainage 0.000. Cross-sections downstream of the EFPC branch are also shown in gray in Figure 14.

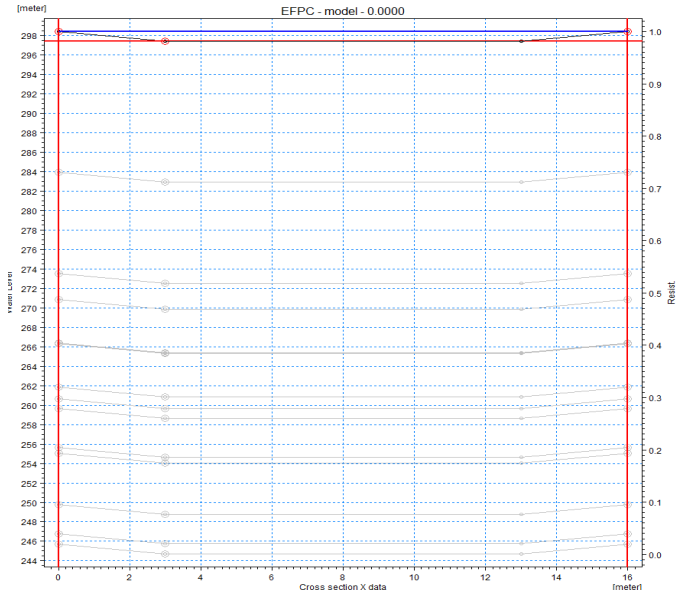

Figure 14. Detailed schematic of river cross-section for EFPC at chainage 0.000 and subsequent chainages downstream.

4.9 ECO Lab

The activated ECO Lab module within the advection component of rivers and lakes currently contains 6 state variables, 11 auxiliary variables, 16 constants, 15 processes, 3 forcing, and 11 derived outputs. The description of the ecosystem state variables is formulated via a series of ordinary coupled differential equations describing the rate of change of each state variable within the ecosystem. Mercury, adsorbed mercury, dissolved mercury in sediment, adsorbed mercury in sediment, suspended solids, and mass of sediment constitute the state variables. Model constants account for the organic-carbon partitioning coefficient, desorption rate in both water and sediment, the fraction of organic carbon in suspended solids and sediment, thickness of the water film, the ratio between the thickness of diffusion layer in sediment, factor for diffusion as a byproduct of bioturbation, molecular weight of heavy metal, density and porosity of dry sediment, settling velocity of suspended solids, resuspension rate, particle production rate, and

critical current velocity for sediment resuspension. The forcing used to represent external variables affecting the ecosystem under analysis includes the current speed, total water depth, and thickness of the computational layer. These components are summarized in the table below.

Table 4. Summary of ECO Lab input.

State Variables	Value	Constants	Value
Mercury	0.01 mg/l	Organic-carbon partitioning coefficient	50000 l/kg
Adsorbed mercury	0.1 mg/l	Desorption rate in water	1 day^{-1}
Dissolved mercury in sediment pore water	0.1 g/m^2	Desorption rate in sediment	0.1 day^{-1}
Adsorbed mercury in sediment	10 g/m^2	Fraction of organic carbon in SS	0.1
Suspended solids	50 mg/l	Fraction of organic carbon in sediment	0.2
Mass of sediment	10000 g/m^2	Thickness of water film	0.1 mm
Forcing		Mole weight of heavy metal	92 g/mole
Thickness computational grid layer	2 m	Density of dry sediment	250 kg/m^3 bulk
Total water depth	8 m	Porosity of sediment	0.8 m^3 H_20 / m^3 Bulk
Current speed	0.2 m/s	Settling velocity of SS	0.1 m/day

In previous years, the sediment transport module was calibrated by Cabrejo and Malek-Mohammadi for the Y-12 Model using an extensive collection of historical records of mercury and total suspended solids (TSS) at Station 17. During the calibration process they considered four parameters that directly affect the concentration of TSS in the water column. These parameters consisted of critical current velocity, settling velocity, resuspension rate, and particle production rate. Sensitivity and uncertainty analysis on each of the parameters mentioned above were extensively performed for the micro-scale model (Y-12) based on available data at Station 17. Since Station 17 is also the only station in the EFPC Watershed model with sufficient data to allow for a comparison between field and simulated values; the significant parameters were selected

from those studies and the values were directly applied to the EFPC Watershed model without extensively investing resources and time in sensitivity and model calibration.

4.10 Assumptions and Limitations

The EFPC Watershed model is subject to a series of assumptions originating primarily from the internal computational generalizations made by the software developers and those inherent to the specific model developed. For example, the software was designed by DHI to disregard density variability within the flow medium. Flow movement is restricted in a direction parallel to the reach bottom. In the software, flow medium movement perpendicular to flow direction is disregarded.

Assumptions pertaining specifically to this case study are rooted in the limitations presented as a byproduct of limited data availability. For example, the ability of the model to simulate the hydrology and transport of mercury at the watershed scale is specifically limited by the geologic variability of the site and the lack of data available to characterize these matrix structures. Per the DOE's 1994 Remedial Investigation Report, groundwater flow for shallow intervals; extending to approximately 100 feet below ground surface, is dominated by interconnected fractures and solution conduits. In such cases where groundwater flow and discharge occur rapidly the contaminants are predicted to be flushed through the system. At intermediate intervals between 100 and 328 feet below the surface, well interconnected zones present a viable environment for plumes to develop. At intervals more than 328 feet in depth the presence of flow zones becomes less frequent. As a result of limited data availability, the model's geologic component was generalized as a 2 layer (upper and lower) aquifer system. This

assumption does not account for fissure conduits present in certain sections of the watershed.

The heterogeneity of the surface or overland features within the domain area also serves as a limiting factor. Certain empirical parameters were set to apply over the entire watershed area. Another limitation of the model is that the precipitation data represents seasonal variability but is not reflective of the spatial variability to which the watershed may be subjected to given a hydrological event. Although the application of the rainfall time-series throughout the watershed is not highly reflective of the spatial dynamics of a hydrological event it currently represents the best means with which to simulate this item.

The capabilities of the mercury transport module within the EFPC watershed model are also limited as it pertains to the development of TMDL studies. It must be taken into account that the direct link between the importance of mercury speciation to the observed concentrations in fish tissue and water quality standards needs to be better established. Fish tissue concentration is related to methyl mercury rather than total mercury. The differences in time and space patterns associated with methyl mercury are ultimately dependent on intricate, inter-connected and interacting transport and transformation processes. The lack of available data for the various phases of mercury in the water column does not allow for a comparison of simulated dissolved and adsorbed mercury concentrations.

An important model limitation is that errors are cumulative throughout the modules. For example, the differences between the observed and simulated flow in the MIKE SHE module is transferred throughout the rest of the modules. Therefore, the mercury mass

rate curves generated take into account and thus accumulate errors carried over from flow and transport modules.

5. RESULTS AND DISCUSSION

A variety of simulations were executed with the purpose applying the recently modified model for flow and mercury in the development of total maximum daily loads study components for the domain area. The term; total maximum daily load, is defined in section 303 (d) of the U.S. Clean Water Act (1972) as the maximum amount of both point and non-point pollutant sources that a body of water can receive while still meeting water quality standards. A TMDL combines the sum of all point source loads known as waste load allocations (WLA) and non-point source loads known as load allocations (LA) with a margin of safety (MOS) that accounts for the uncertainty between the pollutant loads and the receiving water quality. The aforementioned relationship is described by the equation below:

$$TMDL = \Sigma WLA + \Sigma LA + MOS \qquad \text{(Equation 43)}$$

In the past, TMDL efforts for the site have included an extensive analysis of recorded water quality data at outfall points regulated by the National Pollutant Discharge Elimination System. The objective of this study in developing mercury mass rate curves as a partial TMDL analysis tool for EFPC is to understand the contribution of resuspended mercury and how this loading or mass rate curves compare to water quality standards. Efforts associated with this research focus on identifying the percent reduction in resuspended mercury loading or percent reduction of the mercury mass rates at Station 17 necessary to meet designated water quality criterion.

Flow and mercury mass rate curves represent a valid tool for the analysis of data within the TMDL development process. A flow duration curve reveals the relationship between the magnitude of the flow and the frequency in a particular stream [**34**]. Flow duration curves created from averaged data were constructed by ranking available flow data from high to low. The rank position was used to calculate a plotting position also known as the exceedance probability [**34**]. Load duration curves are typically developed by multiplying the daily mean flow by the measured concentration of contaminant. In the present case study, load duration curves have been termed mercury mass rate to avoid confusion with point-source and non-point source pollutant loading. The mercury concentrations considered in this study are not releases of mercury but rather represent mercury that is already present in stream sediment and water and mobilized by stream flow or during hydrological events. Thus, mercury mass rate has been deemed a more appropriate term. Mercury mass rate is calculated very similarly by considering daily mean flow and a measured concentration of total suspended solids or mercury at a point in time.

The model network is shown in Figure 15. Field stations considered are shown (EFK 23.4/Station 17, 03538250, 03538273, 03538270, and 03538673) as well as their model computational counterparts (EFPC 3209.9, EFPC 03538250, BC 8728.87, BC 7700.06, BC 6168.82). The discharge and mercury time-series; depicted in the subsequent sections, reveal variations in discharge and mercury concentrations at various points throughout EFPC and BC being primarily driven by hydrological events.

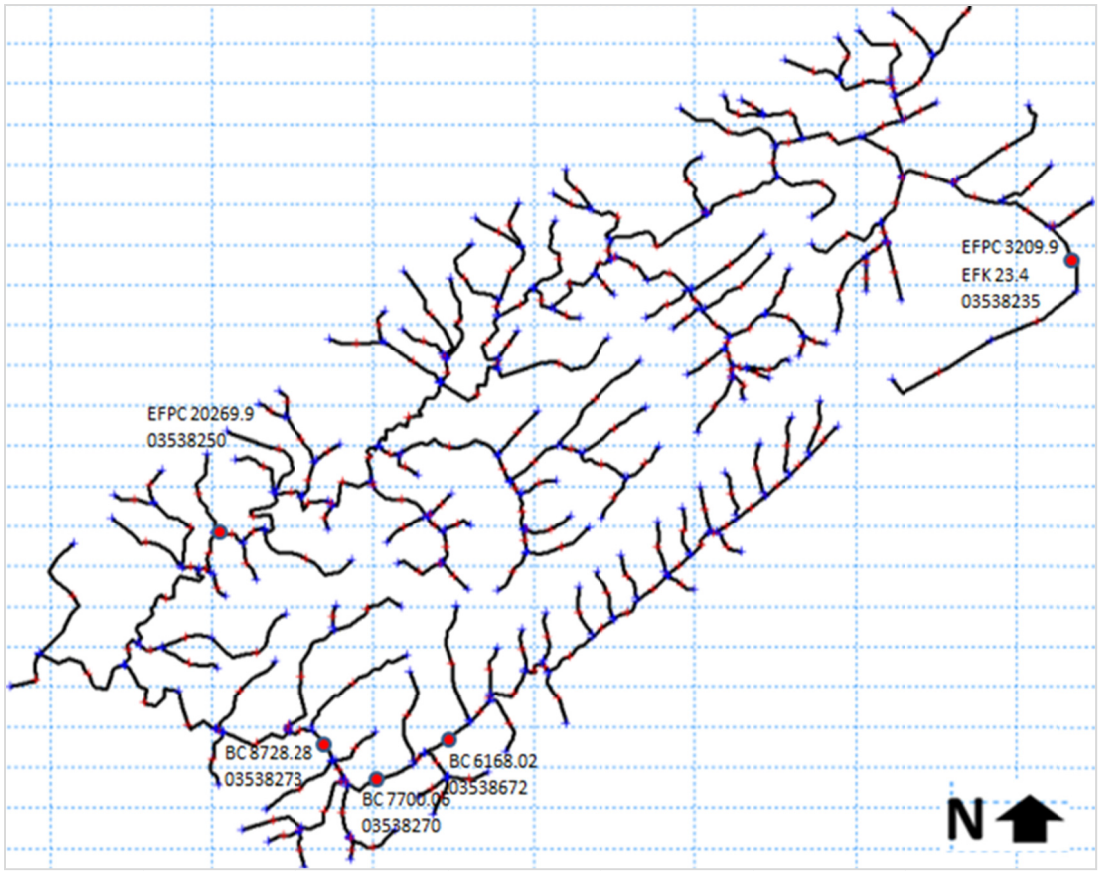

Figure 15. Model network highlighting the stations discussed in the results.

5.1 Overview of Flow Module Results

Flow simulations were set to a period from 7/12/1991 through 1/1/2005. This 13.5-year period contains a range of hydrologic conditions that include low and high stream flows. Simulated flow time-series are shown in Figure 16. Discharge time-series depicting the simulated flow at EFPC 3209.9 and EFK 23.4/Station 17 is shown in Figure 17. The simulated discharge time-series for EFPC 3209.9 exhibited a 22.6% difference in average when compared to field records at Station 17. In reality, flow at Station 17 is not solely dependent upon hydrological events that magnify discharges at a given time. This station is heavily influenced by discharges from regulated outfalls. Discharges from such regulated outfalls can be a contributing factor; amplifying the differences between

computed and observed average flow as well as variability in observed and simulated peak flows at Station 17 and EFPC 3209.9. This area has been subjected to flow augmentation in past remediation attempts. Without considering approximately a 0.28 m^3/s flow augmentation, the simulated flow at EFPC 3209.9 is not expected to have a good fit with observed data from Station 17. At a minimum the flow augmentation scenario needs to be implemented to ensure correlation between the simulated and observed base flow. Discrepancies among the computed and observed average flow is smaller at other points throughout the watershed. For example, downstream EFPC at computational node EFPC 20731.6, the average flow was 1.22 m^3/s while the recorded value for USGS station 03538250 was 1.41 m^3/s. In this case, a 13.5% error between computed and observed average flow values was exhibited. The model reveals general trends consistent with measured data.

Simulated average flow for BC at chainage 8728.28, 7700.06, and 6168.82 were 0.279 m^3/s, 0.215 m^3/s, and 0.156 m^3/s, respectively. This was comparable to the observed average flow of 0.253 m^3/s, 0.212 m^3/s, and 0.143 m^3/s for USGS stations 03538273, 03538270, and 03538672 respectively. The average flow increases downstream EFPC and BC. Similarly, time-series for computed discharges at BC 7700.06 were compared to USGS station 03538270 and are shown in Figure 20. Observed and computed discharges at this station show a much better match in which the base flow is captured by the model.

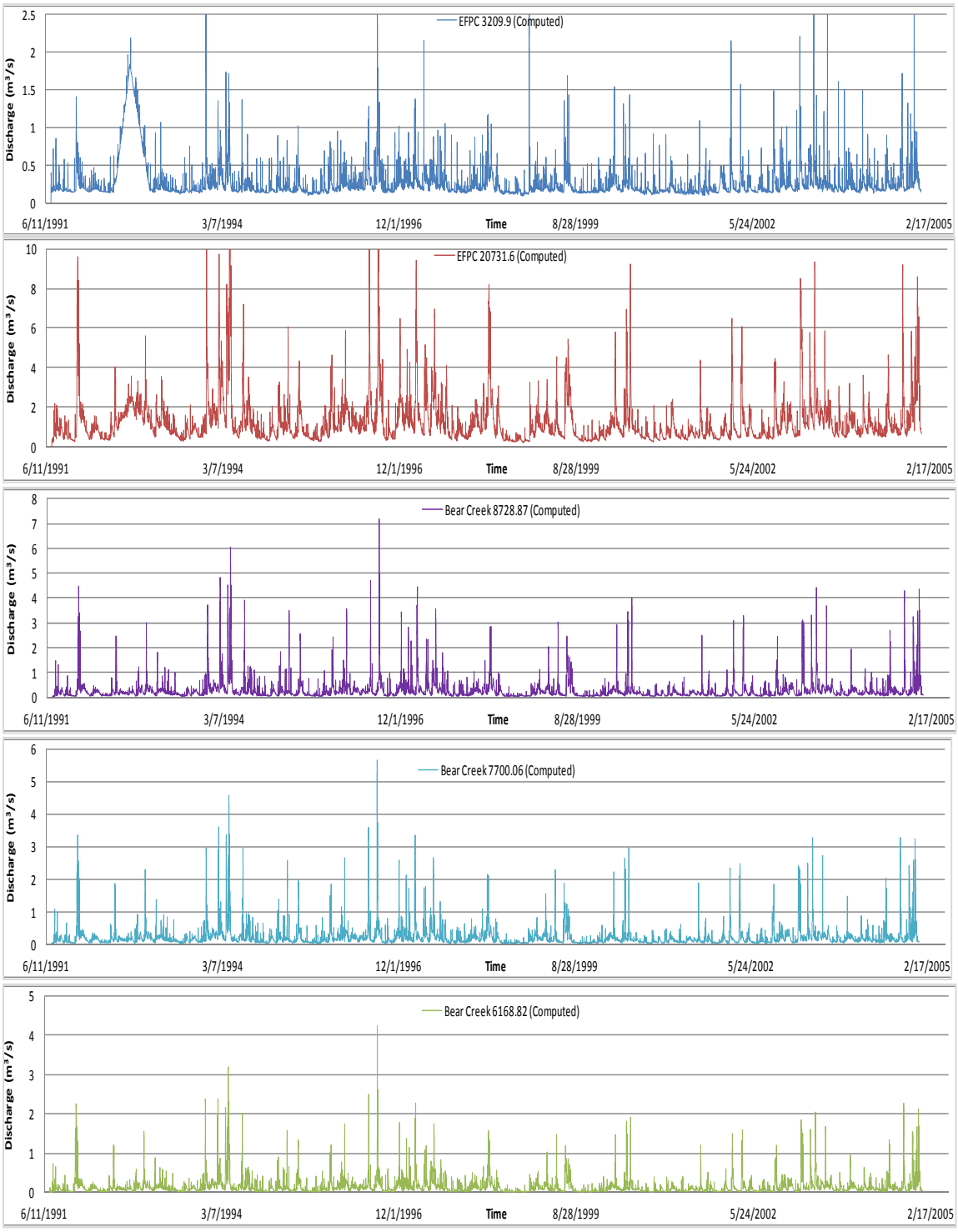

Figure 16. Computed discharges downstream EFPC and BC for various model nodes(EFPC 3209.9, EFPC 20731.6, BC 20731.6, BC 8728.87, BC 7700.06, and BC 6168.82).

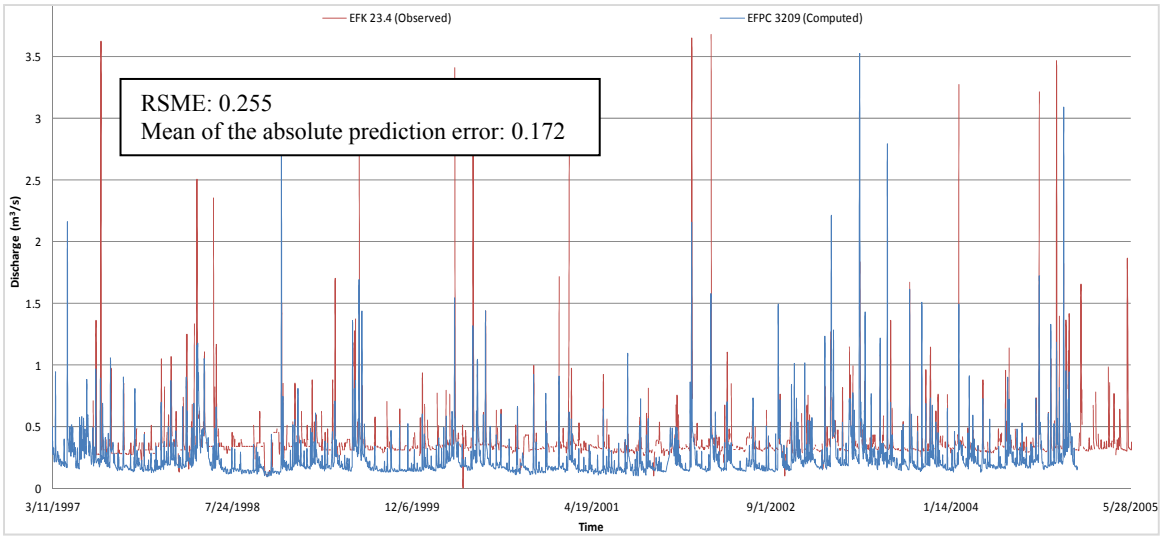

Figure 17. Comparison of discharges time-series at EFPC 3209.9(computed) and EFK 23.4 (observed).

The root mean square error (RSME) has been calculated for the time-series presented in this study in order to measure the average magnitude of the error. The RSME value for each time-series is depicted in the graphic. The difference between the simulated and the corresponding observed or field value was squared and then averaged over the sample data. The square root of the average was then taken. The RSME attributes a relatively large weight to errors.

Flow duration curves for EFPC and BC were constructed from daily flow measurements taken at each station considered. The flow duration curves for various stations are shown in Figure 18, Figure 19, and Figure 21 through Figure 23. These graphics represent the cumulative distribution of daily discharges arranged to show percentage of time specific flows were exceeded during the period of record. The underlying concept behind the cumulative distribution of flow duration curves attributes that the highest daily mean flow during this period is never exceeded and the lowest daily mean flow is always equaled or exceeded. The flow duration curves were divided into

five flow regimes based on a percent exceedance. These included high flows (0-10%), moist conditions (10-40%), mid-range flows (40-60%), dry conditions (60-90%), and low flows (90-100%).

Portions where the simulated flow duration curve represents a good or bad fit with the observed are noted in the figures that follow. With each probability exceedance curve developed for flow duration, mercury concentration, and mercury mass rate a summary of average flow, concentration, or mass rate is provided per flow regime and summarized in tabular format below the graph. The difference between the simulated and observed average per flow regime is also noted. The flow duration curves; Figure 18, Figure 19, and Figure 21 through 23 reveal the model's ability to best simulate flow or discharges during high flow, moist-conditions, and mid-range flows. Dry conditions and low flow regimes establish a greater margin of error and numerical instability.

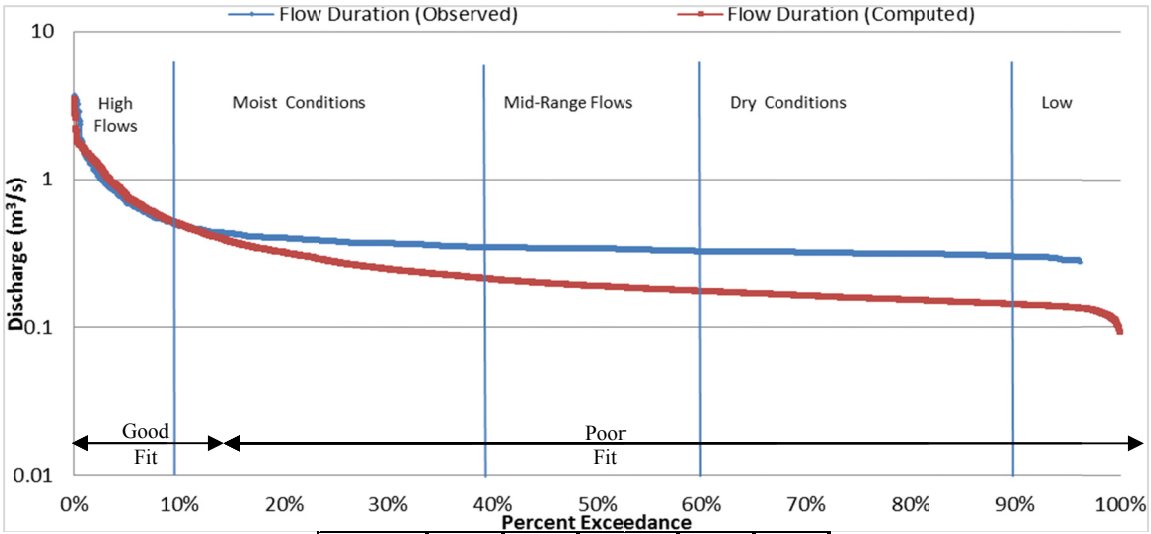

Average Flow (m^3/s)	High	Moist	Mid-Range	Dry	Low
Simulated	0.9370	0.2962	0.1896	0.1577	0.1328
Observed	0.9349	0.3861	0.3360	0.3134	0.2616
Averages Difference	0.0021	0.0899	0.1464	0.1557	0.1288

Figure 18. Comparison of flow duration curves for EFPC 3209.9 (computed) and EFK 23.4 (observed).

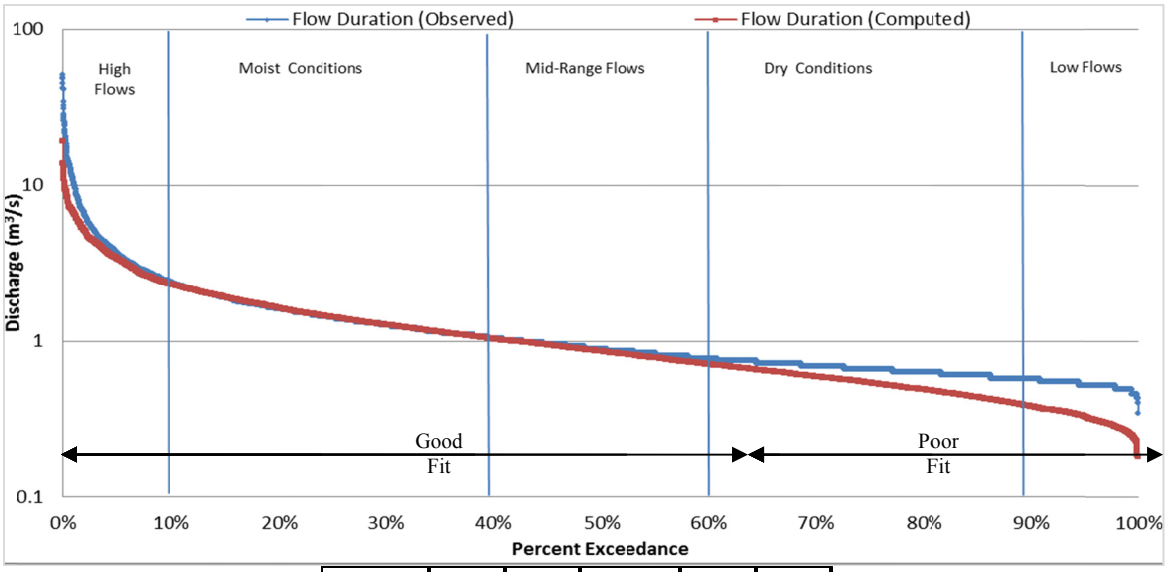

Average Flow (m^3/s)	High	Moist	Mid-Range	Dry	Low
Simulated	4.0445	1.5029	0.8628	0.5416	0.3205
Observed	5.4531	1.4730	0.8784	0.6530	0.5164
Averages Difference	1.4086	0.0299	0.0157	0.1114	0.1959

Figure 19. Comparison of flow duration curves for EFPC 20269.9 (computed) and 03538250 (observed).

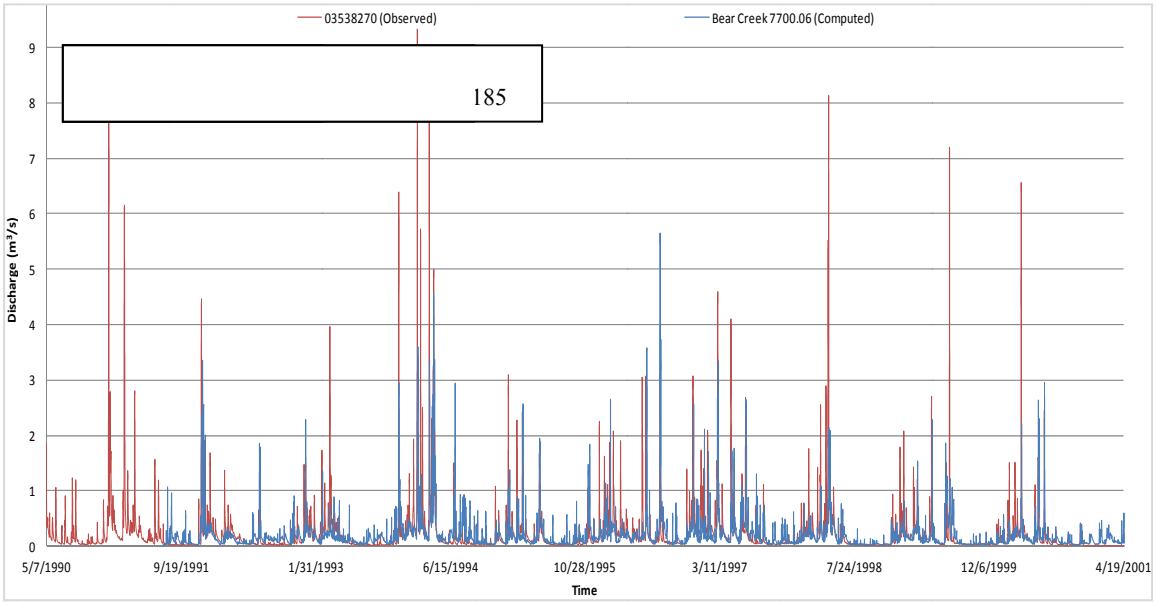

Figure 20. Comparison of discharges time-series at BC 7700.06 (computed) and 03538270(observed).

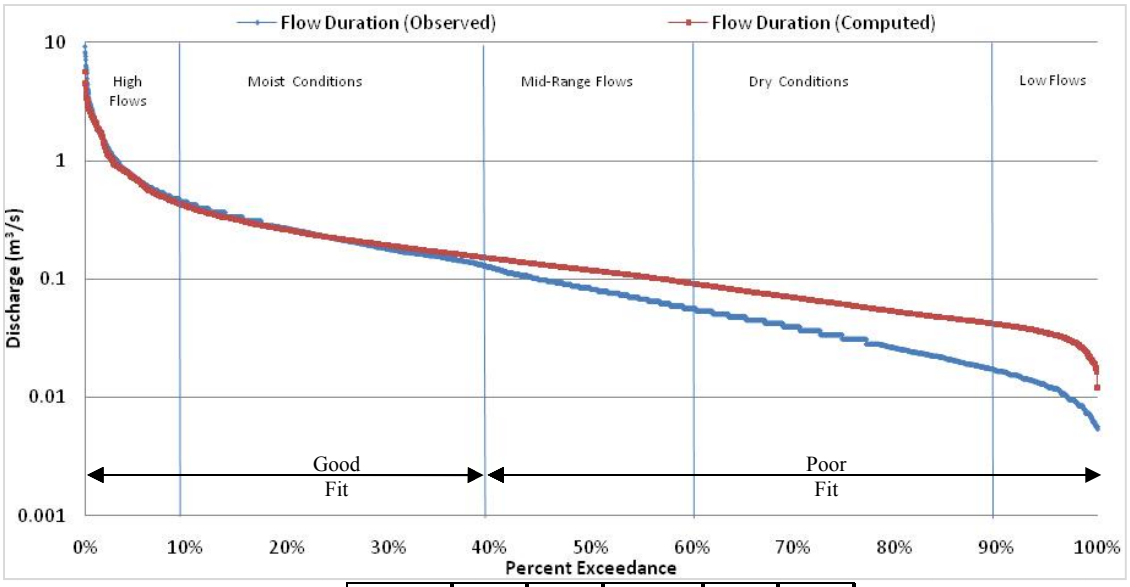

Average Flow (m^3/s)	High	Moist	Mid-Range	Dry	Low
Simulated	1.2825	0.3056	0.1541	0.0811	0.0429
Observed	1.1262	0.2385	0.0851	0.0337	0.0121
Averages Difference	0.1563	0.0671	0.0690	0.0474	0.0307

Figure 21. Comparison of flow duration curves at BC 7700.06 (computed) and 03538270(observed).

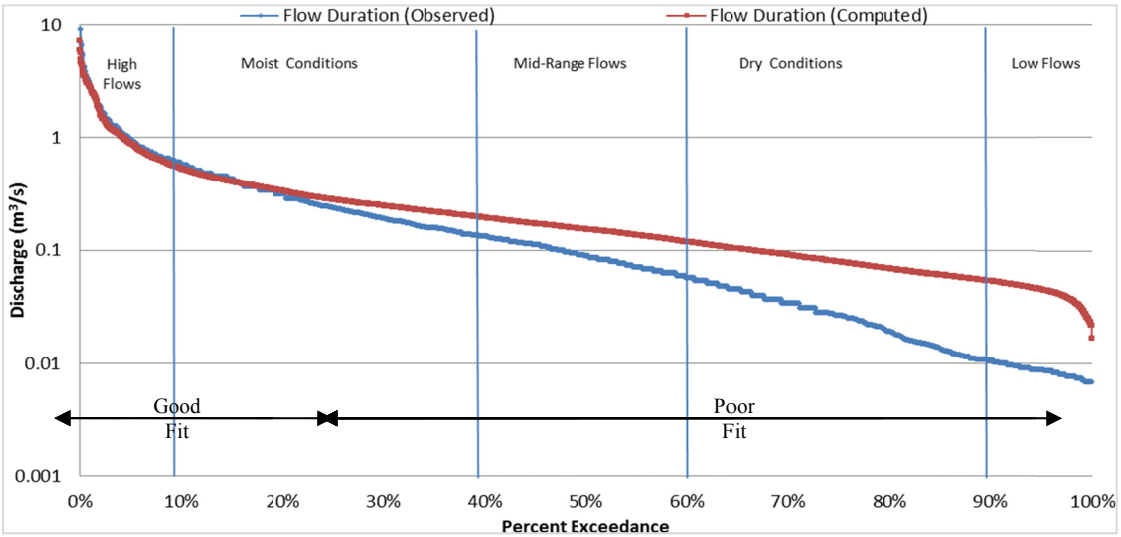

Average Flow (m^3/s)	High	Moist	Mid-Range	Dry	Low
Simulated	1.2825	0.3056	0.1541	0.0811	0.0429
Observed	1.4367	0.2738	0.0910	0.0285	0.0086
Averages Difference	0.1542	0.0318	0.0631	0.0527	0.0342

Figure 22. Comparison of flow duration curves for BC8728.87 (computed) and 03538273 (observed).

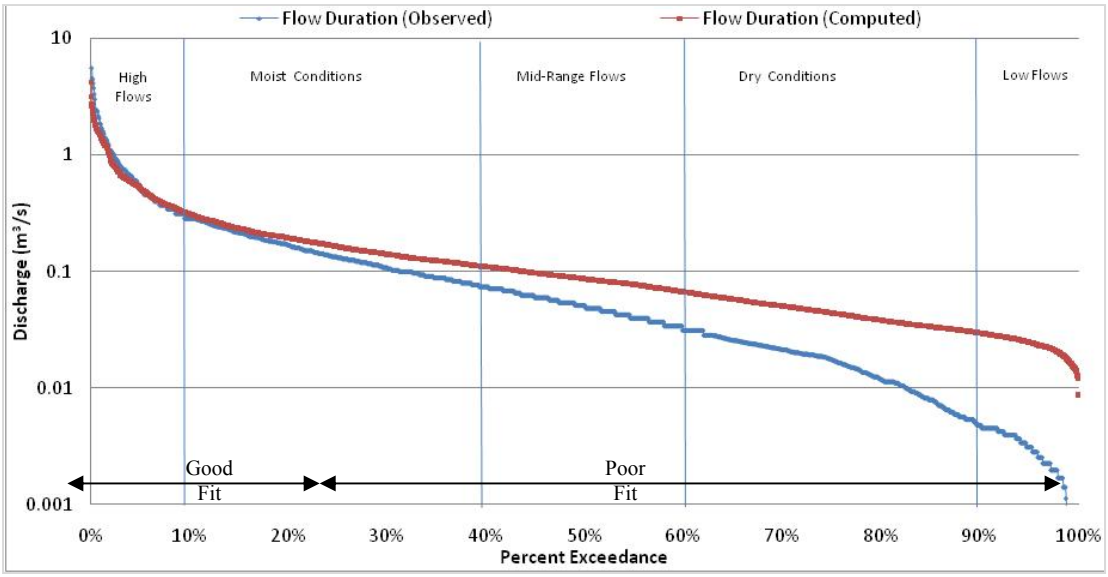

Average Flow (m^3/s)	High	Moist	Mid-Range	Dry	Low
Simulated	0.6950	0.1756	0.0871	0.0452	0.0238
Observed	0.8324	0.1470	0.0509	0.0171	0.0029
Averages Difference	0.1374	0.0286	0.0362	0.0282	0.0209

Figure 23. Comparison of flow duration curves at BC 6168.82 (computed) and 03538673(observed).

5.2 Water Quality Module Results

This section describes components of a preliminary TMDL primarily focused on identifying trends in mercury mass rate curves and quantifying the percent reduction in resuspended mercury mass rates necessary to meet the water quality criterion mandated for the site based on various water user classifications. TMDL components were developed for EFPC based on available water quality data and the application of the model. In accordance with the approach implemented in previous studies; where applicable, total maximum daily loads, waste load allocations, and load allocations are expressed as the percent reduction in flow or mercury concentrations required to maintain the desired target levels of mercury concentrations in fish tissue.

Designated water use classifications for EFPC encompass a wide range. Among these are the ability to sustain fish and aquatic life, irrigation, livestock watering and wildlife, and recreation. In the case of recreation use, a water quality standard of 51 parts per trillion (ppt) total mercury concentration in surface water has been suggested by TDEC, EPA, and DOE. For the protection of fish and aquatic life from toxic inorganic substances the State of Tennessee Water Quality Standards suggested a water quality criterion of 770 ppt. There is also the ROD target of 200 ppt for the Station 17 proposed by DOE. A specific water quality criterion has not been designated yet for irrigation, and livestock watering and wildlife designated uses. Water quality criteria for EFPC are summarized in the table below.

Table 5. Mercury concentration limits per designated usage classification.

Usage Classification	Mercury Concentration (ppt)
Recreation	51
Fish and aquatic life	770
Irrigation	Not Available
Livestock watering and wildlife	Not Available

The EPA currently recommends a water quality criterion for methyl mercury expressed as a fish tissue concentration value of 0.3 milligrams methyl mercury per kilogram of wet-weight fish tissue. Per the EPA, a fish tissue residue water quality criterion for methyl mercury is more appropriate than a water column-based water quality criterion. However, since the direct link between the EPA's fish methyl mercury water quality criterion and the available water quality mercury concentration data for stations in the watershed were difficult to associate the TMDL comparison was based on the most stringent water quality criterion per usage classification. The most stringent water usage

classification was employed and used to establish target levels for TMDL reductions at Station 17.

5.2.1 Time-series of Mercury Concentrations

Simulated mercury time-series are shown in Figure 24 for computational nodes downstream EFPC and BC that overlap with field stations. Simulated average mercury concentrations for BC at chainage 8728.28, 7700.06, and 6168.82 were 1.6 μg/L, 2.2 μg/L, and 2.9 μg/L, respectively. Mercury concentrations appear to decrease upstream BC. The slightly higher average mercury concentration of 2.9 μg/L computed at BC 8728.28 could be attributed to its proximity to EFPC as previous studies hypothesize on the potential of mercury particulates to be carried downstream during extreme hydrological events. In the case of EFPC 3209.9 and observed Stations 17 the simulated and observed mercury concentration do not present a perfect fit. Better correlation between the observed and computed mercury concentration peaks is needed. Figure 25 provides visual information about the close match between observed and computed mercury concentration at Station 17/EFK 23.4. Figure 26 showcases measured discharges and mercury concentration as a function of time in an attempt to identify trends among the two.

Based on the simulation results, it appears that the majority of the mercury in the creek is in the adsorbed form. Shown in Figure 27, approximately 75.2% of the total mercury is in the adsorbed form and 24.8% is estimated to be as dissolved mercury. A more focused time-series shown in Figure 28, highlights fluctuations for the year 2000. This pattern emphasizes the importance of suspended particles and its direct connection to the total mercury concentration in the creek. As shown in Figure 27 and Figure 28, the

streambed pore water within the reach contains very high concentrations of dissolved mercury often exceeding 100 ppt. Dissolved mercury in sediment pore water contributes to the high mercury concentration in the creek water through diffusive transport and pore-water recirculation. This occurs as higher flow in the river suspends both the mercury-laden particulates and the highly contaminated trapped water in sediment pores to the creek water. These findings are consistent with studies that associate floodplain with wet weather, high flow events, as oppose to the headwater flux which seem to occur under base-flow conditions [**6**].

These results are not only consistent with findings from the Y-12 micro-scale model but are also confirmed by field investigations performed by ORNL in previous years. Issues of confidentiality and the lack of public data available to compare the various phases in which mercury is present at Station 17 did not allow for comparison or calibration of simulated dissolved and adsorbed mercury concentrations to field records in this specific case.

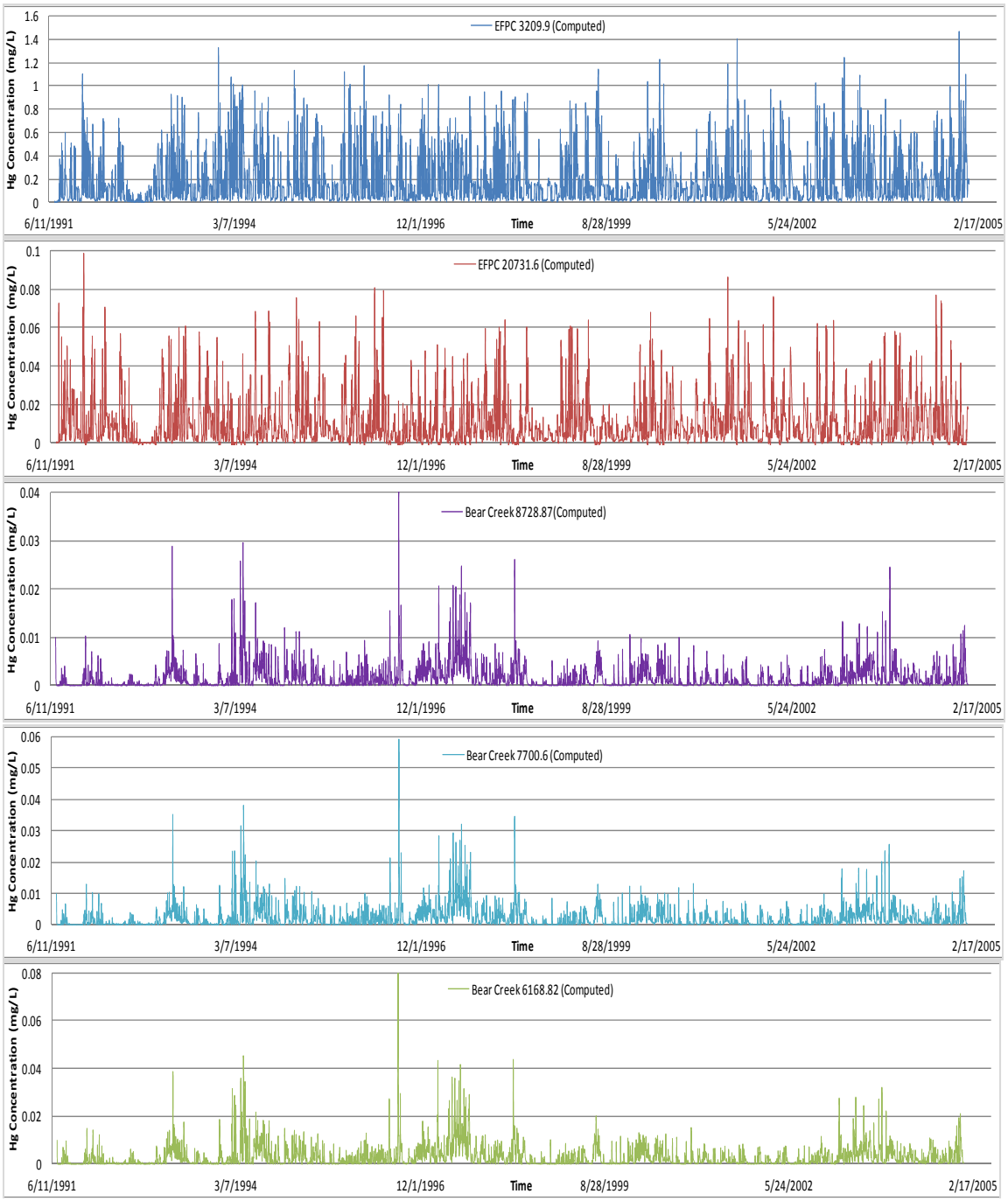

Figure 24. Computed mercury concentrations downstream EFPC and BC for various model nodes (EFPC 3209.9, EFPC 20731.6, BC 20731.6, BC 8728.87, BC 7700.06, and BC 6168.82).

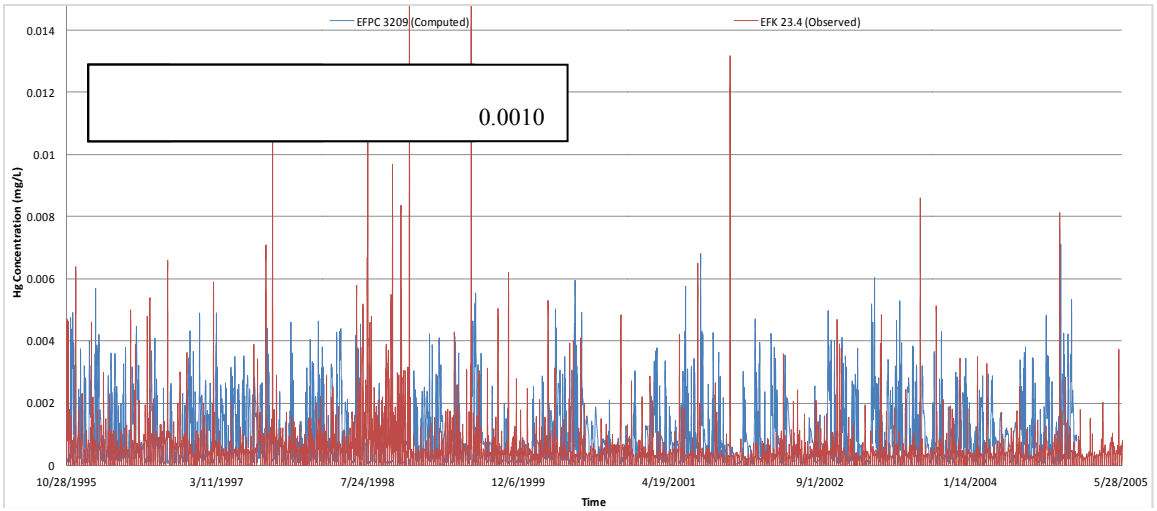

Figure 25. Comparison of mercury time-series at EFPC 3209.9 (computed) and EFK 23.4 (observed).

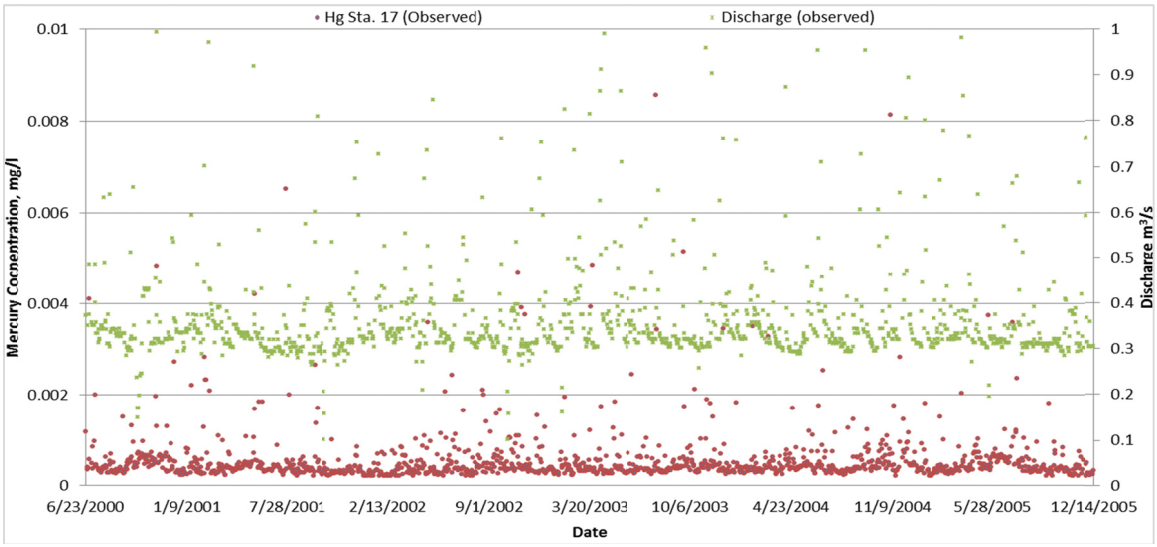

Figure 26. Measured mercury concentrations and discharges at Station 17.

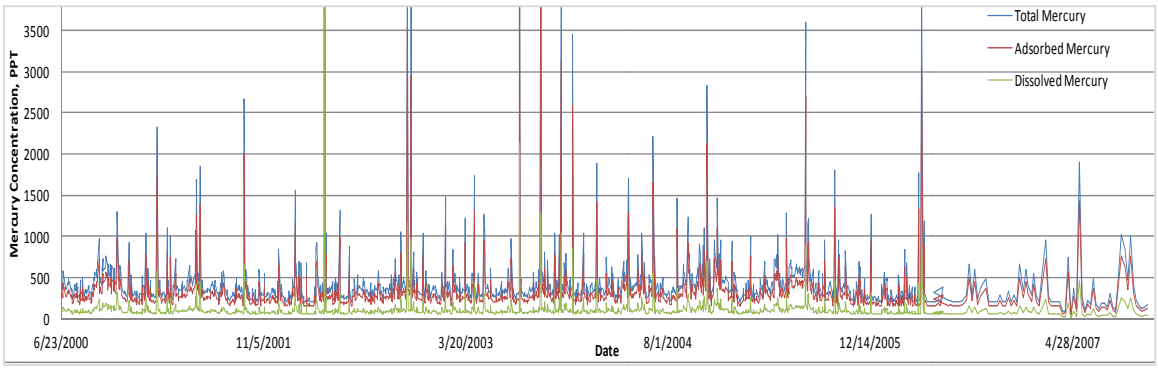

Figure 27. Total adsorbed and dissolved mercury concentration time-series for a simulated period starting at year 2000.

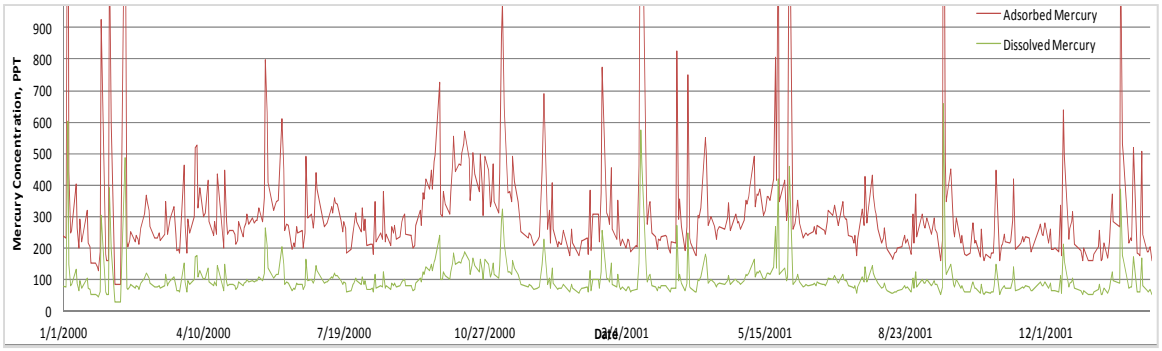

Figure 28. Simulated adsorbed and dissolved mercury concentration time-series for year 2000.

5.2.2 Probability Exceedance Curves for Mercury and TSS

Probability exceedance curves are a classical way for regulators to understand the system in terms of the various flow regimes exhibited. Figure 29 shows the probability exceedances for computed and recorded mercury concentrations for EFPC 3209.9 and EFK 23.4.

The daily flow rates and observed concentration were used to obtain mercury mass rate estimates in an attempt to identify seasonal trends, compare one location to another, and serve as a future tool for the development of water quality goals. Computed and observed mercury mass rates were thus created for the previously discussed field and model stations. These images are shown in Figure 30 through Figure 33. The mercury mass rate curves for model station EFPC 3209.9 and field station EFK 23.4 provides a general trend consistent with the one previously revealed by the flow duration curves. For the loads, similarly to the discharges, the model is best able to simulate the observed for high flow, mid-range flow, and moist conditions. The mercury mass rate appears to be attenuated downstream EFPC, shown in Figure 31. This pattern is not of significance at BC; Figure 32, as the variations of load duration curves is minor throughout BC.

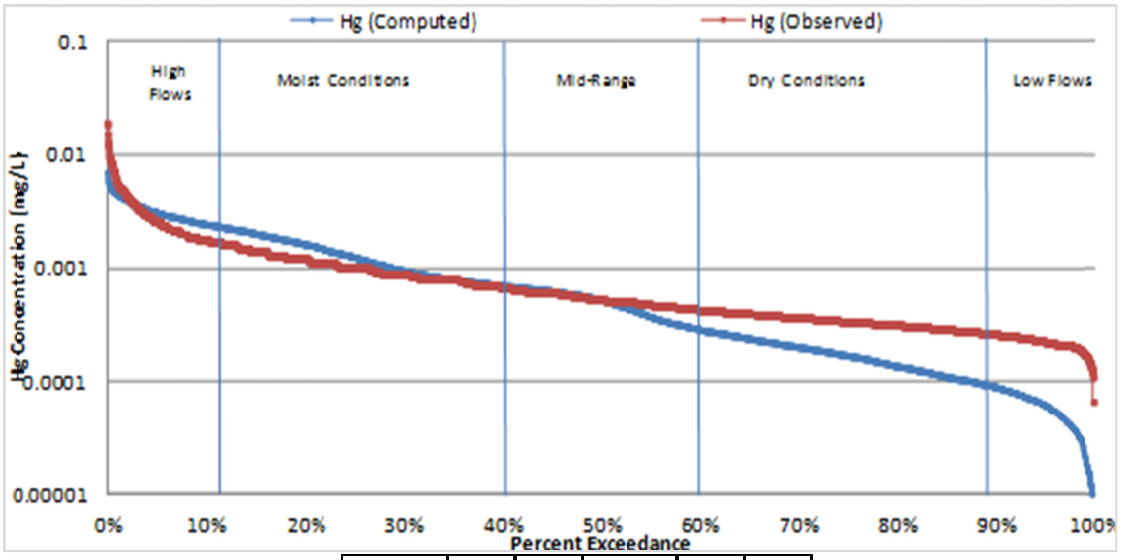

Average Concentration (mg/L)	High	Moist	Mid-Range	Dry	Low
Simulated	0.0033	0.0014	0.0005	0.0002	0.0001
Observed	0.0034	0.0011	0.0005	0.0003	0.0002
Averages Difference	0.0001	0.0003	0.0000	0.0001	0.0001

Figure 29. Comparison of mercury concentration probability exceedances for EFPC 3209.9 (computed) and Station 17 (observed).

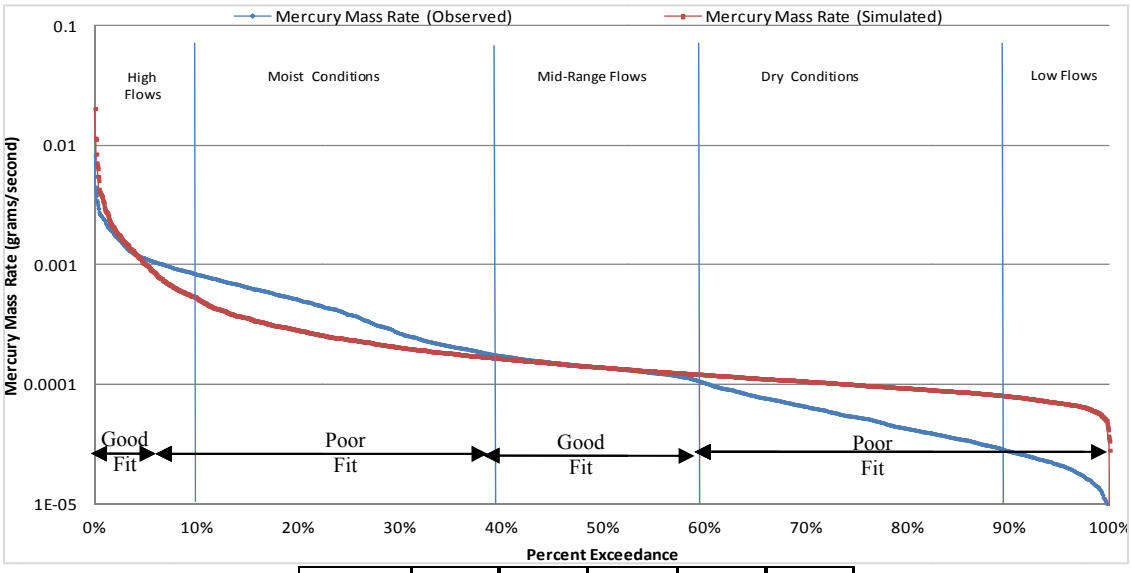

Average Concentration (mg/L)	High	Moist	Mid-Range	Dry	Low
Simulated	0.001681	0.000274	0.000142	0.000101	0.000069
Observed	0.001440	0.000436	0.000142	0.000059	0.000021
Averages Difference	0.000241	0.000163	0.000001	0.000042	0.000049

Figure 30. Comparison of mercury mass rate curves for EFPC 3209.9 (computed) and Station 17 (observed).

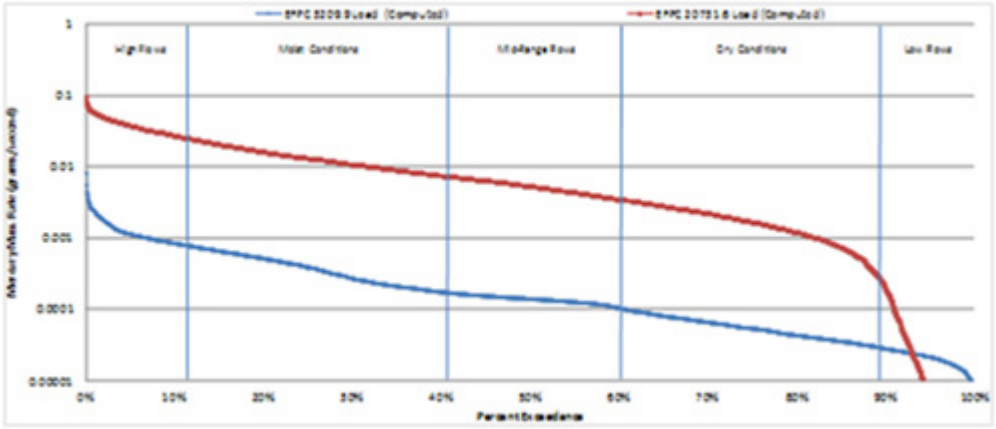

Figure 31. Comparison of mercury mass rate curves downstream EFPC.

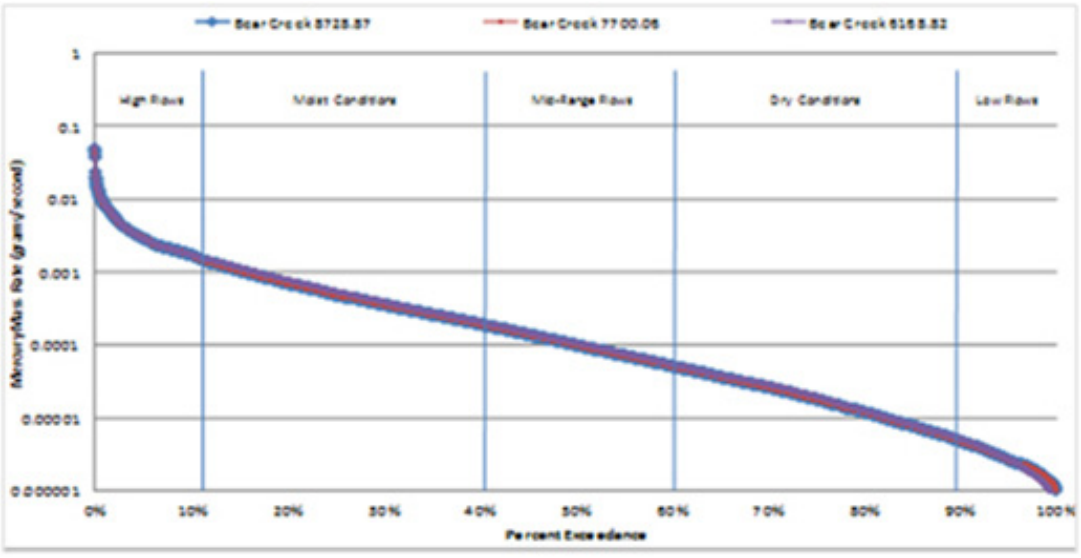

Figure 32. Mercury mass rate curves downstream BC.

Total suspended solids patterns were also investigated for Station 17. The same process applied for analyzing the flow and mercury time-series, generating probability exceedance curves, and loads were implemented when evaluating total suspended solids. Figure 31 compares recorded and computed total suspended solids and mercury load duration curves for different flow conditions and reiterates the observation established by Figure 27 and Figure 28. The resuspension of mercury-laden fine particulates during high flow conditions (i.e., the wet seasons) plays a significant role in the enhancement of local concentration of mercury along the creek.

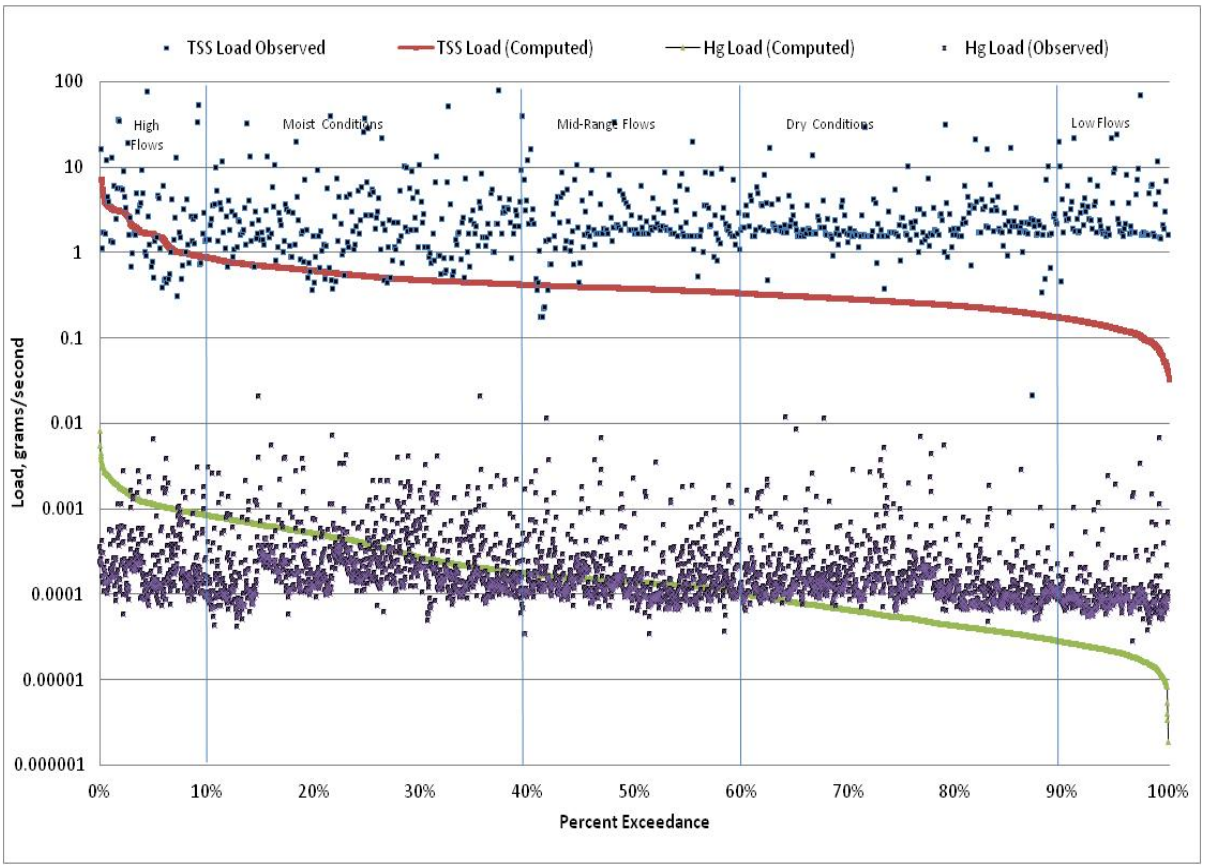

Figure 33. Observed and computed TSS and mercury mass rate curves for Station 17.

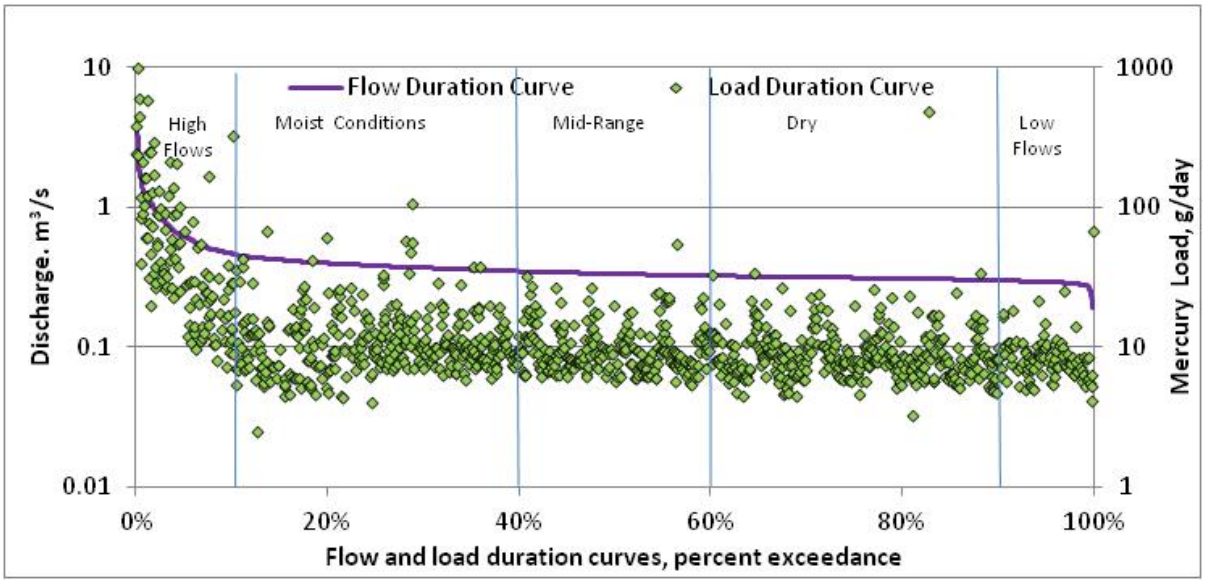

Figure 34. Comparison of flow and load duration curves at Station 17.

5.2.3 Station 17 Target TMDL

The target for the TMDL analyses is the numeric water quality criterion for the pollutant of concern; mercury in this case, for the specified EFPC waterbody. The target concentration was summarized based on the detailed description of water uses and regulations established by the EPA, DOE, and the Tennessee Department of Environment and Conservation. These numeric water quality targets were translated into TMDLs through the loading capacity or as defined by EPA "the greatest amount of loading received without violating water quality standards". Several target load-duration curves were generated for EFPC by multiplying the mercury target concentration of 51, 200, and 770 ppt to each ranked flows. These target mercury load duration curves are shown in the figure below.

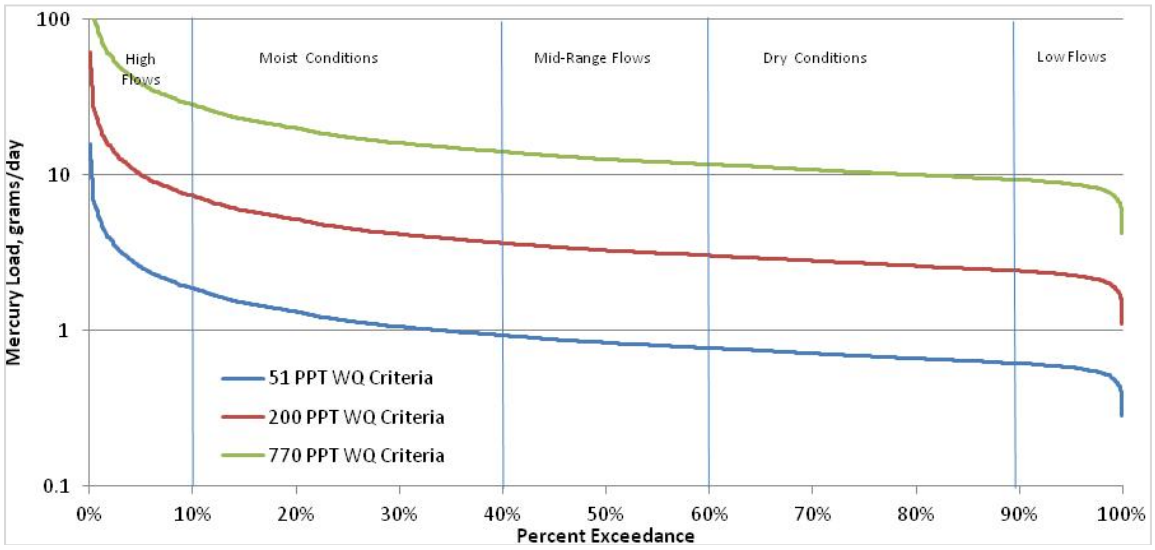

Figure 35. Target mercury load duration curves for 51, 200, and 770 ppt water quality criterion.

Available water quality data for Station 17; encompassing a 10 year period, was utilized to compute the percent reduction required to decrease the concentration from the observed mean considering a 95 percent confidence interval (CI) to the desired target

level. A total of 2,286 samples were considered. All recorded values exceeded the mercury concentration of 51 ppt necessary to meet the recreational use classification. Only 203 of the 2286 samples; in other words, 8.89% of the samples exceeded the 770 ppt criterion required to sustain fish and aquatic life but the majority of the mercury concentrations recorded exceeded the 200 ppt established by the DOE ROD.

Table 6 summarizes the statistical parameters such as the mean, minimum, standard deviation, the 90% CI, and the 95% CI used in calculating the percent reduction required. The percent reduction was calculated as the difference between the mean and the water quality criteria; considering a confidence interval, and divided by the mean with the incorporated confidence interval. This relationship is shown below by equation 44.

Table 6. Target TMDL percent reductions at Station 17.

No. of Samples	Minimum	Mean	Standard Deviation	Criterion 1	Criterion 2
2286	66.10	495.25	668.91	51	770
No. of Samples Exceeding Criterion 1	**No. of Samples Exceeding Criterion 2**	**95% CI**	**Mean + 95% CI**	**90% CI**	**Mean + 90% CI**
All	203	27.42	522.67	23.01	518.26

$$\%\mathrm{Re}duction = \frac{(Mean + Confidence\_Interval) - (Criterion)}{(Mean + Confidence\_Interval)} \qquad \text{(Equation 44)}$$

Based on the equation above, a 90.24% reduction in mercury loading is required at Station 17. It must be noted that this percent reduction was based solely on data from one station, if additional stations or more data were to be considered or disclosed then it is possible that the percent reduction could change. Figure 36 shows how the probability exceedance for mercury loading computed from observed flows and mercury concentrations compare to the standard target mercury mass rate or loading. The average loading at each flow regime is also shown as the dashed red line. Figure 36 also shows the standard water quality criteria compared to the simulated mercury loading for which

the required percent reduction was applied. As can be observed from Figure 37 the percent reduction applied places the simulated loading within the range of the 51 ppt water quality criteria and below the 200 ppt standard mandated by the DOE ROD.

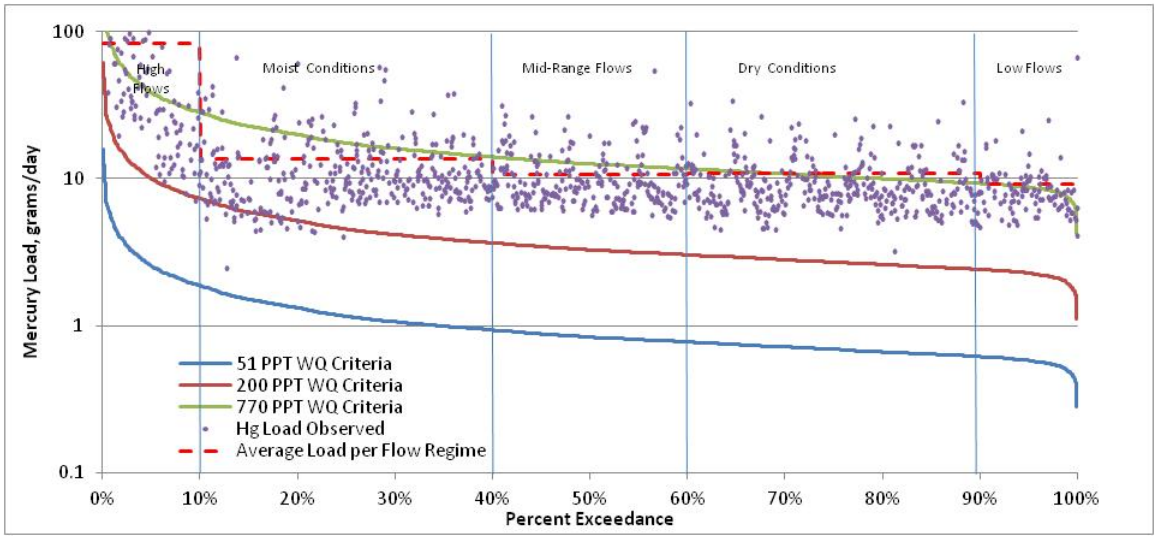

Figure 36. Comparison of target TMDLs and recorded mercury load at station 17.

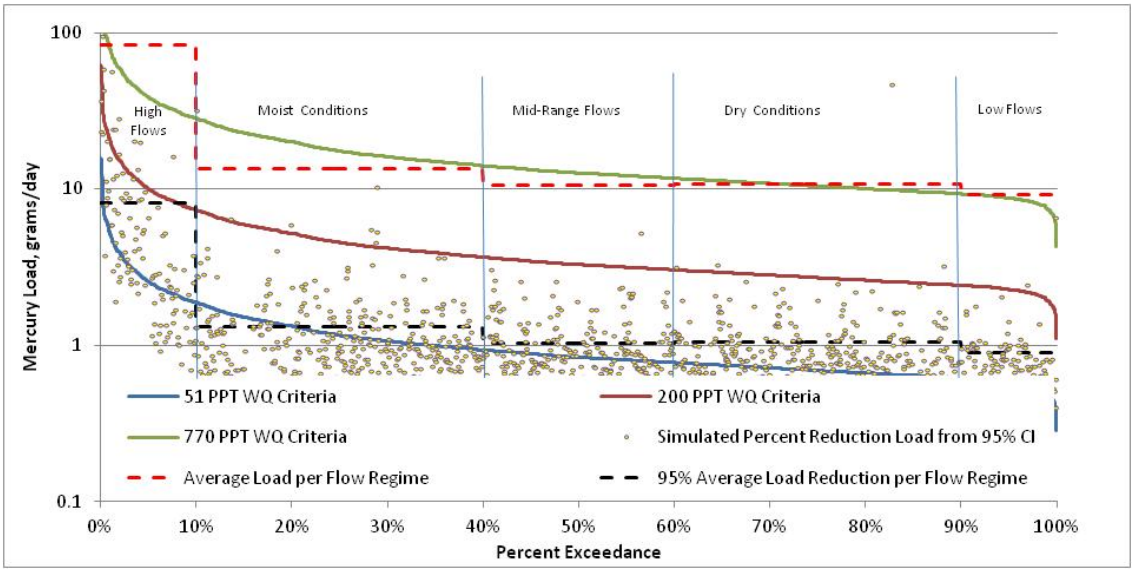

Figure 37. Comparison of simulated mercury loading with applied percent reduction and target TMDLs.

6. CONCLUSIONS

This study has been able to enhance previous versions of the model by considering the most significant parameters and processes of flow and mercury transport for the study site and combining the processes of advection and dispersion within a sedimentation (ECO Lab) module at the EFPC Watershed model scale. The objectives of this thesis were met through the successful integration of this module to enhance the simulation of mercury transport and in the demonstration of the application of the model to the mercury TMDL analysis for the project site in the EFPC watershed.

Modeling software MIKE SHE, MIKE11, and ECO Lab were thus combined in a comprehensive package that models the flow and transport of mercury in exchange with sediment. The application of the enhanced models includes an analysis of spatial and temporal patterns stimulated by variations of selected properties of the sub domain. The impact of sedimentation on the fate of mercury was assessed through a series of simulations and using the sedimentation layer module (ECO Lab); this module addresses the dissolved mercury in the water, the adsorbed mercury concentration on suspended matter, the dissolved mercury in sediment pore water, and the adsorbed mercury in the sediment.

In the application of the model to the EFPC watershed, previous modeling efforts, which originally included only UEFPC, were extended to include the entire EFPC, down to station EFK 6.4 and the BC. The model is capable of simulating the entire hydrological cycle. Water quality, transport, and sediment related parameters were updated based on DOE experimental reports and journal publications to include observed data of flow, stage, and

mercury concentrations in soil, surface water, groundwater and sediments at Station 17 as well as the stations previously mentioned.

Simulations were executed for a range of input parameters to correlate stochastic hydrologic events with mercury distribution patterns and TSS patterns at Station 17. The simulations were analyzed using a range of techniques, primarily comparative schematics of time-series plots, probability exceedance curves, and mercury mass rate curves.

Based on the patterns exhibited throughout various observed and computed probability exceedance curves for flow and mercury, it can be concluded that the model is a good predictor for the wetter regimes. Under the comparison conditions of this study the model simulated values best mimic the observed during high, moist, and mid-range flows. But it certainly fails to effectively simulate in order of magnitudes during the low flow and dry conditions regimes. Although mercury mass rate curves appear to be attenuated downstream EFPC the same cannot be concluded of BC as it exhibits no significance difference between the mercury loading upstream and downstream. Furthermore, results also show that the majority of the mercury in the creek is in the adsorbed form; accentuating the importance of suspended particles and its direct connection to the total mercury concentration in the creek. Even though mercury concentrations during high flood events decrease due to dilution; post hydrological events, the mercury concentration levels are restored. Standard mercury loads probability exceedances were developed based on established limits for the site and a 90.24% reduction in loading appears to be required at Station 17.

The modeling was intended to aid in the development of flow duration curves and mercury loads probability exceedances for selected stations where applicable. The model is

meant to serve as a useful remediation tool since the site was characterized using relevant historical records for precipitation, groundwater levels, and river discharges obtained from OREIS and ORNL databases, which were incorporated into the model in the form of boundary or calibration conditions. The incorporation of the ECO Lab module should better characterize the mercury processes in the EFPC environment since mercury species are known to diffuse from contaminated sediment pore water to creek water in the form of diffusive transport.

7. RECOMMENDATIONS

Improvements can be made to the study in several aspects. For instance, since the study is performed at a watershed scale it might be beneficial to consider the development and implementation of site-specific modeling applications to smaller areas at contaminated buildings and pipes. A more thorough understanding and modeling of the connections between concentrations of inorganic mercury precursors and methyl mercury concentration is also needed to better predict future trends of mercury transport at the site. In this thesis research, the EPA water quality limits previously mentioned and based on water usage classification were used to establish a comparison between simulated and recorded mercury loading. An additional recommendation to improve the understanding of the EFPC system is to more specifically apply the model to understand the bioavailability and bioaccumulation in fish in order to establish a more direct connection between water quality and the DOE ROD set fish tissue concentration value of 0.3 milligrams methyl mercury per kilogram of wet-weight fish tissue for the site.

REFERENCES

[1] DOE (Department of Energy), "Record Decision for Phase II: Interim Source Control Actions in Upper East Fork Poplar Creek Characterization Area, Oak Ridge, Tennessee", 2006.

[2] DOE, "Report on the Remedial Investigation of the Upper East Fork Poplar Creek Characterization Area at the Oak Ridge Y-12 Plant", Oak Ridge, Tennessee, Volume 1, 1998.

[3] Turner, R. R., and Southworth, G. R., "Mercury-Contaminated Industrial and Mining Sites in North America: An Overview with Selected Case Studies in Mercury Contaminated Sites". *Springer-Verlag*, 1999.

[4] Oak Ridge National Laboratory (ORNL), "Conceptual Model of Primary Mercury Sources, Transport Pathways, and Flux at the Y-12 Complex and Upper East Fork Poplar Creek, Oak Ridge, Tennessee", 2011.

[5] Han, F. X., Shiyab, S., Chen, J., Su, Y., Monts, D. L., Waggone,r C. A., and Matta, F. B., "Extractability and Bioavailability of Mercury from a Mercury Sulfide Contaminated Soil in Oak Ridge, Tennessee, USA", *Water Air Soil Pollution*, 194, 67-75, 2008.

[6] Southworth, G., Greeley, M., Peterson, M., Lowe, K., and Kettelle, R., "Sources of Mercury to East Fork Poplar Creek Downstream from the Y-12 National Security Complex: Inventories and Export Rates, Oak Ridge, Tennessee", 2010.

[7] ORNL, Applied Research Initiative. http://www.esd.ornl.gov/romic_afrc/field_ characterization.shtml, February 2013.

[8] Brooks, S. C., and Southworth, G. R., "History of Mercury use and Environmental Contamination at the Oak Ridge Y-12 Plant", *Environmental Pollution*, 219-228, 2011.

[9] Tennessee Department of Environment and Conservation (TDEC) Division of Water Pollution Control Planning and Standards Section, "2008 303 (d) List", 2008.

[10] Liao, L., Selim, H. M., and DeLaune, R. D., "Mercury Adsorption-Desorption and Transport in Soils", *Journal of Environmental Quality*, 38, 1608-1616, 2009.

[11] Cabrejo, E., "Mercury Interaction with Suspended Solids at the Upper East Fork Poplar Creek, Oak Ridge, Tennessee.," Florida International University, Environmental Engineering Department, Miami, Master Thesis 2011.

[12] Morel, F. M., Kraepiel, A. M., and Amyot, M., "The Chemical Cycle and

Bioaccumulation of Mercury", *Annual Review of Ecology and Systematics*, 29, 543-566, 1998.

[13] Miller, C. L., Southworth, G., Brooks, S., and Gu, B., "Kinetic Controls in the Complexation between Mercury and Dissolved Organic Matter in a Contaminated Environment", *Environmental Science Technology*, 43, 8548-8553, 2009.

[14] Parkpoin, P., Thongra-ar, W., DeLaune, R., and Jugsujinda, A., "Adsorption and Desorption of Mercury by Bangpakong River Sediments as Influenced by Salinities", *Journal of Environmental Science and Health*, 36 (5), 623-640, 2001.

[15] Malek-Mohammadi, S., Tachiev, G., Cabrejo, E., and Lawrence, A., "Simulation of Flow and Mercury Transport in Upper East Fork Poplar Creek, Oak Ridge, Tennesse", *Remediation*, 119-131, 2012.

[16] U.S. Geological Survey, "Mercury in the Environment", Fact sheet 146-00, 2000.

[17] Pant, P. and Allen, M., "Interaction of Soil and Mercury as a Function of Soil Organic Carbon", *Environmental Contamination Toxicology*, 2007.

[18] Brigham, M., Wentz, D., Aiken, G., and Krabbenhoft, D., "Mercury Cycling in Stream Ecosystems Water Column Chemistry and Transport", *Environmental Science Technology*, (43), 2720-2725, 2009.

[19] Environmental Protection Agency (EPA) Council for Regulatory Environmental Modeling, "Guidance on the Development, Evaluation, and Application of Environmental Models", 2009.

[20] DOE, "Record of Decision for Phase I: Interim Source Control Actions in Upper East Fork Popler Creek Characterization Area, Oak Ridge, Tennessee", 2002.

[21] DOE, "Record Decision for Phase II: Interim Source Control Actions in Upper East Fork Poplar Creek Characterization Area, Oak Ridge, Tennessee", 2006.

[22] DOE, "Report on the Remedial Investigation of the Upper East Fork Poplar Creek Characterization Area at the Oak Ridge Y-12 Plant. Volume 1, Oak Ridge, Tennessee", 1998.

[23] Long, S., "An Integrated Flow and Transport Model to Study the Impact of Mercury Remediation Strategies for East Fork Poplar Creek Watershed, Oak Ridge, Tennessee", Florida International University, Environmental Engineering Department, Miami, Master Thesis 2009.

[24] Owens, E. M., Bookman, R., Effler, S. W., Driscoll, C. T., Mathews, D. A., and Effler, A. J. P., "Resuspension of Mercury-Contaminated Sediments from an In-Lake Industrial Waste Deposit", *Journal of Environmental Engineering*, 135, 526-

534, 2009.

[25] EPA, "Mercury Study Report to Congress Volume III: Fate and Transport of Mercury in the Environment", 1997.

[26] North Carolina Department of Environment and Natural Resources, "Total Maximum Daily Load for Mercury in the Cashie River, North Carolina, Public Review", 2004.

[27] Gandhi, N., Bhavsar, S. P., Diamond, M .L., Kuwabara, J. S., Marvin-Dipasquale, M., and Krabbenhoft, D. P., "Development of Mercury Speciation, Fate, and Biotic Uptake (BIOTRANSPEC) Model: Application to Lahontan Reservoir, Nevada, USA", *Environmental Toxicology and Chemisty*, 26 (11), 2260-2273, 2007.

[28] Sorensen, H. R.,. Jacobsen, T. V, Kjelds, J. T., Yan, J., and Hopkins, E., "Application of MIKE SHE and MIKE 11 for Integrated Hydrological Modeling in South Florida," South Florida Water Management District (SFWMD) & Danish Hydraulic Institute (DHI), 2012.

[29] Danish Hydraulic Institute (DHI), "Success Story: Broward County, FL Employs MIKE SHE for Integrated Water Resources Master Plan", http://www.mikebydhi.com/~/media/Microsite_MIKEbyDHI/Publications/Success Stories/MIKE%20by%20DHI%20Success%20Story-MSHE-BrowardCounty.ashx

[30] DHI, "MIKE SHE User Manual", 2012.

[31] DHI, "MIKE 11 Reference Manual", 2012.

[32] Rijn, L. V., "Sediment Transport, Part II: Suspended Load Transport", *Journal of Hydraulic Engineering*, 110 (11), 1613-1641, 1984.

[33] DHI, "ECOLAB Short Scientific Description", 2012.

[34] EPA, "Development of Duration-Curve Based Methods for Quantifying Variability and Change in Watershed Hydrology and Water Quality", 2008.

[35] Yin, Y., Allen, H., and Huang, C. P., "Kinetics of Mercury (II) Adsorption and Desorption on Soil", *Environmental Science and Technology*, 496-502, 1997.

APPENDICES

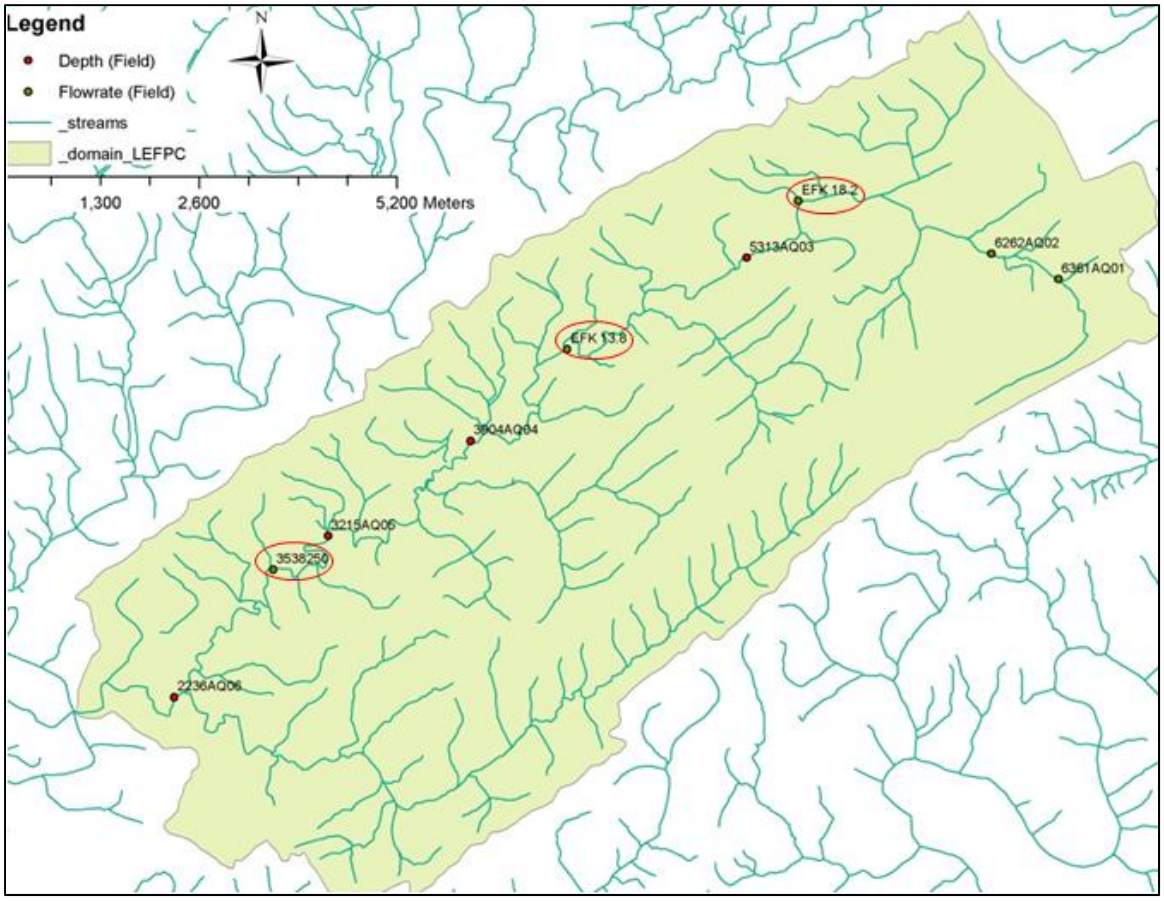

Figure 38. Highlighted stations represent flow data observation points added to the model as time-series

Table 7. EFPC model network branches.

Name	Downstream Chainage	Downstream Connection Name	Downstream Connection Chainage
BC-A-N01	2627.00852	Bear Creek	9274.97319
BC-A-S01	1731.03357	Bear Creek	8228.22922
Bear Creek	12393.1962	EFPC	23342.328
Branch100	570.515326	Bear Creek	1708.63916
Branch101	645.54787	Bear Creek	1238.53279
Branch102	371.057499	Bear Creek	1994.64616
Branch103	367.130677	Bear Creek	2873.2586
Branch104	676.627975	Bear Creek	502.095608
Branch105	738.47401	Bear Creek	855.648999
Branch106	320.135532	EFPC	17698.0082
Branch107	494.19464	EFPC	20073.4189
Branch108	337.941501	EFPC	20996.8015
Branch109	272.418154	BC-A-N01	1027.66123
Branch110	928.093627	Bear Creek	7040.48431
Branch111	512.962161	Branch110	505.555117
Branch112	407.512497	Branch110	505.555117
Branch113	915.067283	EFPC	9091.23597
Branch18	623.430043	EFPC	3679.62887
Branch19	767.032449	EFPC	4382.24429
Branch20	1562.3612	EFPC	5085.13617
Branch21	747.976283	EFPC-A-S04	1394.2137
Branch22	479.446328	EFPC-A-N04	2412.89544
Branch23	733.906826	EFPC-A-N04	1365.18116
Branch24	1062.82743	EFPC-A-N04-N01	1475.16897
Branch25	574.90101	EFPC-A-N04-N01	755.286944
Branch26	1349.79425	EFPC	7282.7484
Branch27	305.550978	Branch26	645.560017
Branch28	1385.65267	EFPC	7647.66632
Branch29	411.312158	EFPC-A-S04	1078.92038
Branch30	1220.46903	EFPC	8026.57498
Branch31	1100.44229	EFPC-A-S04	1625.79832
Branch32	1119.24833	Milton Branch	2212.74766
Branch33	640.394531	Milton Branch	2215.26565
Branch34	394.470438	Milton Branch	1906.67759
Branch35	1094.31462	Milton Branch	1906.67759
Branch36	555.989773	Branch37	1241.65263
Branch37	1389.40442	Milton Branch	1417.23759
Branch38	258.90626	Milton Branch	299.935879
Branch39	763.967426	Branch37	998.198308
Branch40	349.971877	Branch37	863.709821

Table 7. EFPC model network branches (Cont.)

Name	Downstream Chainage	Downstream Connection Name	Downstream Connection Chainage
Branch41	306.896242	Branch39	600.112762
Branch42	648.620057	Milton Branch	893.27888
Branch43	410.206634	EFPC	13730.9602
Branch44	341.965487	EFPC	11930.5444
Branch45	345.398656	EFPC	11105.8086
Branch46	1343.24789	EFPC	10541.2185
Branch47	491.932802	Branch46	635.497021
Branch48	1123.56862	EFPC	12342.9044
Branch49	613.000721	EFPC-A-N03	672.619034
Branch50	1074.72944	EFPC-A-N03	1426.07585
Branch51	1674.47658	EFPC	14936.3057
Branch53	1168.69096	Branch51	1362.24078
Branch54	614.27993	Branch51	1308.53024
Branch55	420.959085	EFPC-A-N02	689.961838
Branch56	1506.09017	EFPC	18288.5517
Branch57	349.039006	Branch56	1036.12
Branch58	367.643714	Branch56	376.299345
Branch59	1362.67434	EFPC	18651.3516
Branch60	785.591557	EFPC	18651.3516
Branch61	455.319439	EFPC-A-N01	509.372774
Branch62	1090.51342	EFPC	20466.32
Branch63	1095.59976	EFPC-A-N01	1615.37626
Branch64	1783.7922	EFPC	24812.5811
Branch65	365.341176	Pinhook Branch	877.595397
Branch66	406.584377	Pinhook Branch	1141.96693
Branch67	565.599776	Pinhook Branch	1141.96693
Branch68	625.023043	Pinhook Branch	467.553892
Branch69	710.859381	Gum Hollow Branch	2607.62585
Branch70	604.115881	GHB-A-S05	875.782043
Branch71	646.687734	GHB-A-S05	1162.66811
Branch72	466.240066	GHB-A-S05	1629.21892
Branch73	1553.5932	Gum Hollow Branch	1495.13032
Branch74	957.998954	Branch73	1304.78772
Branch75	565.605786	Branch73	611.384598
Branch76	386.093979	Gum Hollow Branch	3961.40439
Branch77	757.166531	EFPC-A-S01	1940.3623
Branch78	1180.43707	Bear Creek	10308.0545
Branch79	747.814346	Bear Creek	10203.6514
Branch80	656.335209	Bear Creek	8506.0781
Branch81	1061.41327	Bear Creek	8506.0781

Table 7. EFPC model network branches (Cont.)

Name	Downstream Chainage	Downstream Connection Name	Downstream Connection Chainage
Branch82	455.792787	BC-A-S01	813.365846
Branch83	459.796837	Branch82	426.125736
Branch84	1335.56282	Bear Creek	8161.14718
Branch85	287.505808	Branch84	703.608893
Branch86	1598.99258	Bear Creek	8951.6694
Branch87	1219.09375	Bear Creek	7238.97864
Branch88	1504.98443	Bear Creek	6349.44565
Branch89	602.005039	Bear Creek	5917.48305
Branch90	776.620137	Bear Creek	5988.19373
Branch91	508.739969	Bear Creek	5288.30912
Branch92	619.209188	Bear Creek	4969.5992
Branch93	696.968113	Bear Creek	4839.21515
Branch94	628.918276	Bear Creek	4133.97608
Branch95	643.724335	Bear Creek	3766.44731
Branch96	574.72635	Bear Creek	3372.95977
Branch97	643.289247	Bear Creek	2873.2586
Branch98	608.276871	Bear Creek	2496.828
Branch99	568.290615	Bear Creek	2105.09977
EFPC	25485.1953		
EFPC-A-N01	1820.50769	EFPC	21183.8791
EFPC-A-N02	1546.16389	EFPC	14936.3057
EFPC-A-N03	1616.78645	EFPC	12948.7807
EFPC-A-N04	2934.28761	EFPC	6498.75737
EFPC-A-N04-N01	1611.75264	EFPC-A-N04	2100.35832
EFPC-A-S01	2243.13258	EFPC	22905.6146
EFPC-A-S02	1435.42326	EFPC	19750.8333
EFPC-A-S03	1671.92188	EFPC	13831.4589
EFPC-A-S04	2306.03929	EFPC	5746.31448
GHB-A-S05	1829.8496	Gum Hollow Branch	2253.28604
Gum Hollow Branch	4259.9214	EFPC	16319.3026
Milton Branch	3414.31997	EFPC	10778.9293
Pinhook Branch	2016.48484	EFPC	16958.969

Table 8. Network points example for branch BC-A-N01 and BC-A-S01.

X Coordinate	Y Coordinate	Branch	Chainage Type	Chainage
750360	181500	BC-A-N01	System Defined	0
750190	181600	BC-A-N01	System Defined	197.23083
750060	181510	BC-A-N01	System Defined	355.34471
749940	181500	BC-A-N01	System Defined	475.76066
749930	181420	BC-A-N01	System Defined	556.38324
749710	181260	BC-A-N01	System Defined	828.41265
749520	181200	BC-A-N01	System Defined	1027.6612
749420	181100	BC-A-N01	System Defined	1169.0826
749270	181060	BC-A-N01	System Defined	1324.3243
749210	180930	BC-A-N01	System Defined	1467.5025
749120	180790	BC-A-N01	System Defined	1633.9357
749120	180680	BC-A-N01	System Defined	1743.9357
749100	180430	BC-A-N01	System Defined	1994.7344
749180	180140	BC-A-N01	System Defined	2295.5666
748960	180030	BC-A-N01	System Defined	2541.5341
748940	179980	BC-A-N01	System Defined	2595.3857
748950	179950	BC-A-N01	System Defined	2627.0085
748370	178730	BC-A-S01	System Defined	0
748704.07	178836.58	BC-A-S01	System Defined	350.65372
748941.5	178880.67	BC-A-S01	System Defined	592.14686
749120	178750	BC-A-S01	System Defined	813.36585
749230	178740	BC-A-S01	System Defined	923.81946
749390	178820	BC-A-S01	System Defined	1102.7049
749390	178920	BC-A-S01	System Defined	1202.7049
749450	179000	BC-A-S01	System Defined	1302.7049
749520	179290	BC-A-S01	System Defined	1601.0336
749640	179340	BC-A-S01	System Defined	1731.0336

Table 9. EFPC model boundary conditions per branch.

Boundary Description	Boundary Type	Branch Name	Chainage	Boundary ID
Open	Inflow	Bear Creek	0	N/A
Open	Inflow	Branch100	0	N/A
Open	Inflow	Branch101	0	N/A
Open	Inflow	Branch102	0	N/A
Open	Inflow	Branch103	0	N/A
Open	Inflow	Branch104	0	N/A
Open	Inflow	Branch105	0	N/A
Open	Inflow	Branch106	0	N/A
Open	Inflow	Branch107	0	N/A
Open	Inflow	Branch108	0	N/A
Open	Inflow	Branch109	0	N/A
Open	Inflow	Branch110	0	N/A
Open	Inflow	Branch111	0	N/A
Open	Inflow	Branch112	0	N/A
Open	Inflow	Branch113	0	N/A
Open	Inflow	Branch18	0	N/A
Open	Inflow	Branch19	0	N/A
Open	Inflow	Branch20	0	N/A
Open	Inflow	Branch21	0	N/A
Open	Inflow	Branch22	0	N/A
Open	Inflow	Branch23	0	N/A
Open	Inflow	Branch24	0	N/A
Open	Inflow	Branch25	0	N/A
Open	Inflow	Branch26	0	N/A
Open	Inflow	Branch27	0	N/A
Open	Inflow	Branch28	0	N/A
Open	Inflow	Branch29	0	N/A
Open	Inflow	Branch30	0	N/A
Open	Inflow	Branch31	0	N/A
Open	Inflow	Branch32	0	N/A
Open	Inflow	Branch33	0	N/A
Open	Inflow	Branch34	0	N/A
Open	Inflow	Branch35	0	N/A
Open	Inflow	Branch36	0	N/A
Open	Inflow	Branch37	0	N/A
Open	Inflow	Branch38	0	N/A

Table 9. EFPC model boundary conditions per branch (Cont.)

Boundary Description	Boundary Type	Branch Name	Chainage	Boundary ID
Open	Inflow	Branch39	0	N/A
Open	Inflow	Branch40	0	N/A
Open	Inflow	Branch41	0	N/A
Open	Inflow	Branch42	0	N/A
Open	Inflow	Branch43	0	N/A
Open	Inflow	Branch44	0	N/A
Open	Inflow	Branch45	0	N/A
Open	Inflow	Branch46	0	N/A
Open	Inflow	Branch47	0	N/A
Open	Inflow	Branch48	0	N/A
Open	Inflow	Branch49	0	N/A
Open	Inflow	Branch50	0	N/A
Open	Inflow	Branch51	0	N/A
Open	Inflow	Branch53	0	N/A
Open	Inflow	Branch54	0	N/A
Open	Inflow	Branch55	0	N/A
Open	Inflow	Branch56	0	N/A
Open	Inflow	Branch57	0	N/A
Open	Inflow	Branch58	0	N/A
Open	Inflow	Branch59	0	N/A
Open	Inflow	Branch60	0	N/A
Open	Inflow	Branch61	0	N/A
Open	Inflow	Branch62	0	N/A
Open	Inflow	Branch63	0	N/A
Open	Inflow	Branch64	0	N/A
Open	Inflow	Branch65	0	N/A
Open	Inflow	Branch66	0	N/A
Open	Inflow	Branch67	0	N/A
Open	Inflow	Branch68	0	N/A
Open	Inflow	Branch69	0	N/A
Open	Inflow	Branch70	0	N/A
Open	Inflow	Branch71	0	N/A
Open	Inflow	Branch72	0	N/A
Open	Inflow	Branch73	0	N/A
Open	Inflow	Branch74	0	N/A
Open	Inflow	Branch75	0	N/A
Open	Inflow	Branch76	0	N/A
Open	Inflow	Branch77	0	N/A
Open	Inflow	Branch78	0	N/A

Table 9. EFPC model boundary conditions per branch (Cont.)

Boundary Description	Boundary Type	Branch Name	Chainage	Boundary ID
Open	Inflow	Branch79	0	N/A
Open	Inflow	Branch80	0	N/A
Open	Inflow	Branch81	0	N/A
Open	Inflow	Branch82	0	N/A
Open	Inflow	Branch83	0	N/A
Open	Inflow	Branch84	0	N/A
Open	Inflow	Branch85	0	N/A
Open	Inflow	Branch86	0	N/A
Open	Inflow	Branch87	0	N/A
Open	Inflow	Branch88	0	N/A
Open	Inflow	Branch89	0	N/A
Open	Inflow	Branch90	0	N/A
Open	Inflow	Branch91	0	N/A
Open	Inflow	Branch92	0	N/A
Open	Inflow	Branch93	0	N/A
Open	Inflow	Branch94	0	N/A
Open	Inflow	Branch95	0	N/A
Open	Inflow	Branch96	0	N/A
Open	Inflow	Branch97	0	N/A
Open	Inflow	Branch98	0	N/A
Open	Inflow	Branch99	0	N/A
Open	Inflow	EFPC	0	N/A
Point Source	Inflow	EFPC	0	N/A
Point Source	Inflow	EFPC	7.69702308	200
Point Source	Inflow	EFPC	15.1815578	135
Point Source	Inflow	EFPC	28.5337035	134
Point Source	Inflow	EFPC	93.2045032	126
Point Source	Inflow	EFPC	99.9074534	125
Point Source	Inflow	EFPC	144.267419	114
Point Source	Inflow	EFPC	253.302757	113
Point Source	Inflow	EFPC	318.675028	110
Point Source	Inflow	EFPC	364.903089	109
Point Source	Inflow	EFPC	370.037803	102
Point Source	Inflow	EFPC	390.364968	99
Point Source	Inflow	EFPC	459.803948	87
Point Source	Inflow	EFPC	459.803948	88
Point Source	Inflow	EFPC	484.094043	86

Table 9. EFPC model boundary conditions per branch (Cont.)

Boundary Description	Boundary Type	Branch Name	Chainage	Boundary ID
Point Source	Inflow	EFPC	487.198636	83
Point Source	Inflow	EFPC	551.868787	71
Point Source	Inflow	EFPC	582.150378	67
Point Source	Inflow	EFPC	622.587496	62
Point Source	Inflow	EFPC	628.418544	64
Point Source	Inflow	EFPC	632.571374	63
Point Source	Inflow	EFPC	697.070226	58
Point Source	Inflow	EFPC	701.909704	57
Point Source	Inflow	EFPC	716.780429	55
Point Source	Inflow	EFPC	741.47639	51
Point Source	Inflow	EFPC	764.022982	54
Point Source	Inflow	EFPC	785.40445	48
Point Source	Inflow	EFPC	787.82346	47
Point Source	Inflow	EFPC	804.502318	46
Point Source	Inflow	EFPC	820.952263	44
Point Source	Inflow	EFPC	845.446533	42
Point Source	Inflow	EFPC	883.151953	41
Point Source	Inflow	EFPC	933.004587	34
Point Source	Inflow	EFPC	943.002728	33
Point Source	Inflow	EFPC	1020.78772	21
Point Source	Inflow	EFPC	1059.24245	20
Point Source	Inflow	EFPC	1177.78284	19
Point Source	Inflow	EFPC	1347.73701	16
Point Source	Inflow	EFPC	1399.69678	14
Point Source	Inflow	EFPC	1946.26967	6
Point Source	Inflow	EFPC	2050.32925	7
Point Source	Inflow	EFPC	2398.76723	3
Point Source	Inflow	EFPC	2456.77397	2
Open	Q-h	EFPC	25485.2	N/A
Open	Inflow	EFPC-A-N01	0	N/A
Open	Inflow	EFPC-A-N02	0	N/A
Open	Inflow	EFPC-A-N03	0	N/A
Open	Inflow	EFPC-A-N04	0	N/A
Open	Inflow	EFPC-A-N04-N01	0	N/A
Open	Inflow	EFPC-A-S01	0	N/A
Open	Inflow	EFPC-A-S02	0	N/A
Open	Inflow	EFPC-A-S03	0	N/A
Open	Inflow	EFPC-A-S04	0	N/A
Open	Inflow	GHB-A-S05	0	N/A

Table 9. EFPC model boundary conditions per branch (Cont.)

Boundary Description	Boundary Type	Branch Name	Chainage	Boundary ID
Open	Inflow	GHB-A-S05	0	N/A
Open	Inflow	Gum Hollow Branch	0	N/A
Open	Inflow	Milton Branch	0	N/A
Open	Inflow	Pinhook Branch	0	N/A
Closed		BC-A-S01	0	N/A
Closed		BC-A-N01	0	N/A